



Cite this: *Mater. Adv.*, 2021,
2, 7308

Received 12th August 2021,
Accepted 25th September 2021

DOI: 10.1039/d1ma00719j

rsc.li/materials-advances

First transition series metal–organic frameworks: synthesis, properties and applications

Sandeep Kaushal, * Gurmeet Kaur, Jasmeen Kaur and Prit Pal Singh *

Metal organic frameworks (MOFs) have captured immense attention in the last decade, owing to their better adsorption properties as compared to those of organic as well as inorganic materials, like enormous surface area, highly porous nature, tunable pore size, and high stability. Herein, the regular advancements in MOFs of metals of the first transition series, their morphology, properties, synthesis methods, and numerous applications like gas storage, separation, ion-exchange and catalysis have been discussed. The doping of MOFs and their composites has been classified and discussed, in addition to fabrication of MOFs with various types of organic linkers. MOFs have been discussed for their sustainable and convenient use in future. Various characterization techniques confirmed the rigid, porous and fine structure of MOFs.

Introduction

Metal organic frameworks (MOFs) are an evolving class of porous materials fabricated from metal clusters or ions and organic linkers in three-dimensional space.^{1–3} MOFs are attractive materials for both researchers and engineers, owing to their tunable structures and functionality as well as their ever-increasing applications.^{4,5} M. Yaghi is known as the father of MOFs as he fabricated advanced MOFs, zeolitic imidazolate frameworks (ZIFs) and covalent organic frameworks (COFs). Various techniques such as *in situ* synthesis, encapsulation, impregnation, gas phase infiltration, co-precipitation *etc.* are employed for the fabrication of MOFs.^{3–5} In recent years, synthesis of many nanostructured and nano-sized MOFs has been carried out.^{6,7} The transformation in the structure of MOFs is contingent on conditions like pH, molar ratio, solvents and temperature.⁸ MOFs have flexibility⁹ and a diverse range of applications¹⁰ including electrochemical applications,¹¹ gas storage,^{12,13} separation,¹⁴ catalytic activity,^{15,16} heterogeneous catalysis,^{17,18} heavy metal removal,¹⁹ drug delivery,^{20,21} membrane desalination,²² water treatment,²³ electrode materials for supercapacitance,^{24,25} ultrasonics,²⁶ luminescence,^{27,28} energy storage,²⁹ photocatalysis,^{30,31} adsorption,³² sensing,³³ enzyme immobilization,³⁴ bio-medicine,³⁵ solid phase extraction/analytical applications,³⁶ dye/toxic materials removal,^{37–39} coordination chemistry,⁴⁰ optics⁴¹ and optoelectronics which are attracting researchers. There have been reports of more than 20 000 MOFs which are different from each other depending on their design, method of synthesis, structure, pore size, *etc.*

The shape, size and nature of pores in MOFs can be easily altered and this leads to rare chemical adaptability. Most of the reported MOFs have been fabricated from divalent or trivalent 3p metal ions, 3d transition metals and lanthanides whereas the fabrication of MOFs from high-valent metal ions is still a big challenge. Furukawa *et al.*⁴² fabricated MOFs having a covalent bond between metal ions acting as nodes and organic ligands taken as spokes which combine to form open framework structures. The significant advances were also discussed, for constructing higher order mesoscopic superstructures that are composed of nanocrystals. These structures are divided into four categories: zero dimensional structures comprising hollow capsules, uni-dimensional structures like nanorods, bi-dimensional structures classified as thin films, membranes or patterns and three-dimensional structures made up of continuous and enlarged systems.⁴³

Herein, the synthesis, structure and applications of MOFs based on first transition series elements have been discussed. Commonly used organic linkers in the frameworks are fumaric acid, oxalic acid, terephthalic acid, benzene-dicarboxylate, adipic acid, *etc.* In addition to organic linkers, some ionic liquids are also used for the fabrication of MOF composites. The commonly used ionic liquids for fabrication of composites are *N*-alkyl-methyl-imidazolium, *N*-alkyl-pyridinium, tetraalkyl-ammonium, tetraalkyl-phosphonium, *etc.* The reactions of most of the metal ions with numerous organic linkers are feasible and given in Fig. 1 and 2.

Here, we are considering metals of first transition series for fabrication of MOFs. These elements have a partially filled d-subshell or can result in cations with an incomplete subshell with general electronic configuration $(n-1)d^{1-10}ns^{0-2}$. Later in this paper, MOFs of Sc, Ti, V, Cr, Mn, Fe, Co, Ni, Cu and Zn have been discussed. The discussion includes the capability of MOFs

Department of Chemistry, Sri Guru Granth Sahib World University, Fatehgarh Sahib, Punjab, India. E-mail: kaushalsandeep33@gmail.com, dhillonps2003@gmail.com



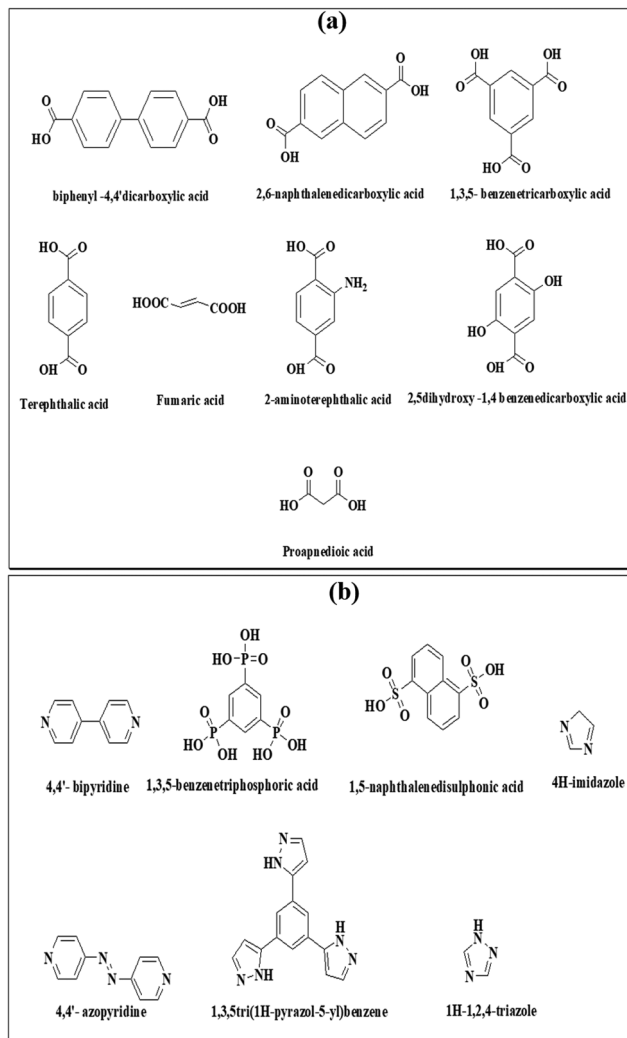


Fig. 1 Organic linkers containing (a) carboxylic functionality and (b) phosphorus, nitrogen and sulphur used for the preparation of MOFs.

for the environmental systems that may include sterilization, gas storage and separation, and gas fuel stockpiling. Thus, MOFs show their advantageous role in energy generation and storage. In this way, MOFs are leading to an ecologically sustainable and convenient future.^{44,45}

Synthetic approaches for metal organic frameworks

Due to their certain functional and structural properties, MOFs have been presently perceived as an extensive collection of porous compounds. These frameworks are formed by connecting organic linkers and metal ion clusters/metal ions. Beyond question, another perception remarkably associated with MOFs conclusive design and properties is the chosen essential structural blocks known as secondary building units (SBUs).⁴⁶ However, various other synthetic approaches and variables like pressure, temperature, pH, time of reaction and solvent should also be scrutinized. Various distinctive synthetic routes *viz.*

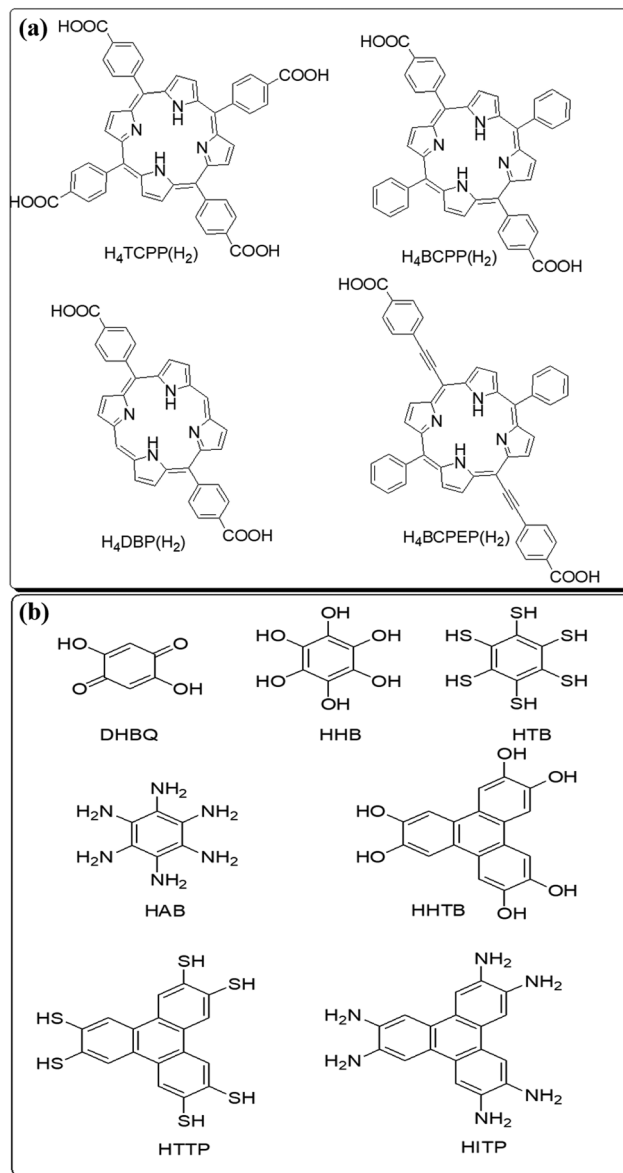


Fig. 2 Organic linkers with (a) conductive linkers and (b) porphyrin-based linkers used for the preparation of MOFs.

hydrothermal/solvothermal, diffusion, electrochemical, mechanochemical, microwave assisted heating and ultrasound can be used to construct MOFs trusting on the subsequent structures and features.^{47,48}

Hydrothermal/solvothermal method

The solvothermal technique is the most utilized strategy for the preparation of MOFs as it gives an assortment of morphologies. In this strategy, the reaction materializes between the metal salt and organic ligand in organic solvents or dissolvable mixtures. Hydrothermal reactions are accomplished at temperatures higher than the boiling point of solvent. It may be inferred that speedy reaction kinetics of hydrothermal reaction allows the construction of even MOF particles with higher crystallinity,

and promptly acquires single crystals. Notwithstanding the advantageous features, this method unquestionably has a few constraints like necessity of solvent antecedents, creation of a lot of solvent waste and possibly harmful treatment of destructive metal salts within the sight of organic liquids.⁴⁹

Slow diffusion method

The diffusion technique brings different species into interaction, step by step: (i) the first strategy is solvent liquid diffusion. In this method, two layers with different densities, the precipitant solvent constituting one layer and the other layer containing the product in a solvent, are formed. At the boundary, formation of crystals takes place by slow diffusion of the precipitant solvent into the other layer; (ii) the second strategy involves the step by step diffusion of reactants by overcoming the physical obstructions. The vital benefit of this technique is that single crystals suitable for XRD analysis can be easily obtained. The more time consuming nature of this method than other notable strategies is its major limitation.⁵⁰

Electrochemical method

In this method, metal ions are released by anodic dissolution into a reaction comprising organic linkers and electrolytes. The electrochemical method is applied for the synthesis of MOF powders on an industrial scale. Some of the advantages of this technique comprise the evading of anions like nitrates from metal salts, low temperature of reaction and tremendously rapid synthesis in comparison to solvothermal synthesis. A contradiction in thermal growth coefficients amongst the distinctive support structure and the MOF prompts this breaking. In this regard, MOFs display a negative thermal expansion coefficient. Therefore, contrasted with the solvothermal method, electrochemical techniques provide more variables for fine tuning by straightforward modification of the voltage.⁵¹

Mechanochemical method

Mechanochemical strategy involves the execution of chemical reaction with the assistance of mechanical power. In this method, chemical reactions and numerous physical phenomena could be carried out by mechanical force. In this method, mechanical cracking of intramolecular bonds is carried out and is followed by chemical synthesis. The main advantage of this method is that the reaction is performed at ambient temperature in the absence of harmful organic solvents. Another significant feature of this method is use of metal salts instead of metal oxides. However, this method has the disadvantage of undesirable product amorphization caused by neat milling.⁵²

Microwave method

Microwave assisted synthesis is a rapid technique for fabrication of MOFs. On irradiation of the reaction mixture with microwaves

for an hour or more, nanosized crystals are formed. The microwave assisted method is an indispensable strategy to perform synthesis at a rapid pace. The advantages of this method include great efficacy, fast reaction kinetics, phase selectivity, uniform particle morphology, particle size reduction, *etc.*⁵³ However, this method usually can't yield crystals with adequate size for single X-ray analysis.⁵⁴

Sonochemical method

In sonochemical synthesis, reaction mixture is exposed to ultrasound waves (20 kHz–10 MHz) and the molecules experience chemical change to yield compounds with innovative morphologies, crystal sizes and distinct properties. Ultrasonic radiation can create high temperatures and pressing factors in the reaction medium. The economical, usually fast, reproducible and environment friendly nature are the main advantages of this method.⁵⁵ Just like microwave method, this method typically can't produce crystals with satisfactory size for single X-ray analysis.

Scandium-based metal organic frameworks

Scandium is the first member of first transition series and has silver white appearance. It may also appear yellow or pink due to different oxidation states of scandium. There is an emerging enthusiasm for utilization of Sc(III) centers for the fabrication of porous frameworks, since it is a moderately light metal which offers high porosity with large specific surface area, high hydrolytic and thermal stability of coordination framework with diverse functional properties and forms stable carboxylate complexes. Despite undeniable advantages and prospects, the science of scandium complexes and, specifically, scandium organic frameworks (SOFs) has inadequately evolved. An impressive limiting component is that scandium is a trace element and, correspondingly, scandium compounds are generally costly.⁵⁶ Barsukova *et al.* reported solvothermal synthesis of three new coordination polymers based on scandium ions and 2,5-furandicarboxylate (fdc^{2-}) ligand *i.e.* $((\text{CH}_3)_2\text{NH}_2)[\text{Sc}(\text{H}_2\text{O})_2(\text{fdc})_2]\cdot 1.5\text{CH}_3\text{CN}$ (1), $((\text{CH}_3)_2\text{NH}_2)[\text{Sc}(\text{fdc})_2(\text{HCOO})]$ (2), and $[\text{Sc}_2(\text{H}_2\text{O})_2(\text{fdc})_3]$ (3). It has been established that these MOFs retain their structure in aqueous media over an extensive pH range of 1–13. Furthermore, compounds 2 and 3 have also shown ligand-centered luminescence.⁵⁷ In another study, properties of Sc- and Ti-based MOFs, $(\text{C}_6\text{H}_3)_2(\text{B}_2\text{C}_4\text{H}_4)_3\text{M}_6$ ($\text{M} = \text{Sc, Ti}$), for storage of H_2 were examined by density functional theory (DFT). It was revealed that each doped Sc atom is capable of adsorbing four H_2 molecules, with average adsorption energy ranging from 0.21 to 0.34 eV.⁵⁸

Similarly, 3D porous bi-metallic frameworks of scandium metal ions along with lithium or sodium metal ions, coordinated to pyrimidine dicarboxylate were synthesized to investigate its capability to arrest CO_2 at room temperature. A heat assisted solvent-free process was established to be most effective, yielding materials with nearly the same adsorption capacities



as anticipated from Grand Canonical Monte Carlo (GCMC) calculations. The synthesized materials possessed high specific surface area, and systematic distribution of alkaline ions in the crystal structure. The ionic conductivity was also enhanced (10^{-4} S cm $^{-1}$) by partial substitution of scandium ions with Li $^{+}$ and Na $^{+}$ ions.⁵⁹ Pillai *et al.* synthesized and explored a series of functionalized scandium terephthalate MOFs for selective CO₂ adsorption. The computational studies revealed that Sc₂(BDC-NO₂)₃ MOFs exhibited exceptional adsorption for CO₂ over N₂ and CH₄, beating the vast majority of MOFs as well as other reported porous materials.

The sample exhibited very good water stability and can be easily regenerated at room temperature under vacuum.⁶⁰ Khan *et al.* introduced scandium-triflate (Sc(OTf)₃) MOFs and carried out adsorptive desulfurization and denitrogenation of fuels. In comparison to sole MOFs, Sc(OTf)₃ MOFs exhibited much better adsorption for benzothiophene (BT) from liquid fuel. Basic quinolone (QUI) was also adsorbed preferentially on acidic Sc(OTf)₃ MOFs (Fig. 3). The improved adsorption might be attributed to interactions between acidic Sc(OTf)₃ and basic adsorbates. The efficiency of the adsorbent was enhanced by solvent washing and thermal treatment.⁶¹

Graham *et al.* fabricated a scandium terephthalate MOF (Sc₂(BDC)₃, BDC = 1,4-benzenedicarboxylate) and its derivative (Sc₂(NO₂-BDC)₃). The as-synthesized MOFs were employed for methanol uptake at high pressure. Diffraction experiments revealed that molecules of methanol occupied two sites, and one site was preferentially occupied in comparison to the other. The likely orientation of methanol molecules was controlled by H-bonding.⁶² Furthermore, Cabello and co-workers utilized variable-temperature infrared (VTIR) spectroscopy to report interactions between carbon dioxide and coordinatively unsaturated MIL-100(Sc) MOFs. The ΔH° value was found to be -48 kJ mol $^{-1}$ which is the highest reported for adsorption of CO₂ on MOFs comprising open metal sites. The corresponding ΔS° value was found to be -178 J mol $^{-1}$ K $^{-1}$ which displayed a positive correlation between ΔH° and ΔS° .⁶³ Similarly, Mitchell *et al.* also reported porous MOFs with scandium and different linkers. The synthesized MOFs were used as catalysts in numerous reactions catalyzed by Lewis acid catalysts which are very

significant in organic synthesis but have not been studied using MOF catalysts.⁶⁴ Arean *et al.* reported the thermodynamics of hydrogen interaction with MIL-100(Sc) MOF with VTIR spectroscopy. The corresponding values of ΔH° and ΔS° were observed to be -11.2 (± 1) kJ mol $^{-1}$ and -120 (± 10) J mol $^{-1}$ K $^{-1}$, respectively, in the temperature range of 80–125 K. The enthalpy for adsorption of hydrogen was observed to be the highest on the MOFs reported so far.⁶⁵

Titanium-based metal organic frameworks

Titanium is viewed as a most interesting contender for the development of MOFs with high chemical stability and structural diversity. Titanium is a tetravalent element in ionic form and is placed just above zirconium in the periodic table. The ionic radius of Ti $^{4+}$ is smaller than Zr $^{4+}$ and hence, Ti $^{4+}$ shows stronger affinity for oxygen. Furthermore, the most attractive characteristic of titanium is its outstanding multifunctionality, typical redox activity, photochemical property and biocompatibility. Titanium-based MOFs exhibit comparatively higher stability in water. Still, the framework of titanium slowly breaks down in water within days which is attributed to the attack of OH $^{-}$ on O-Ti-O bond. An *et al.* enhanced the stability of titanium-based MOFs in water without affecting its other properties by employing Ti-ATA (ATA = 2-aminoterephthalate ion), a titanium-based MOF.⁶⁶ Zhu *et al.* described titanium-based MOFs as a smart subclass of MOF family due to their encouraging stability, properties and inimitable structural features.⁶⁷ Similarly, Zhang *et al.* synthesized Ti-based MOFs, MIL-125 and NH₂-MIL-125 solvothermally. As concentration of Ti was increased, particle size of MIL-125 decreased (Fig. 4). The catalytic properties of MOFs were investigated using H₂O₂ as an oxidant. In the

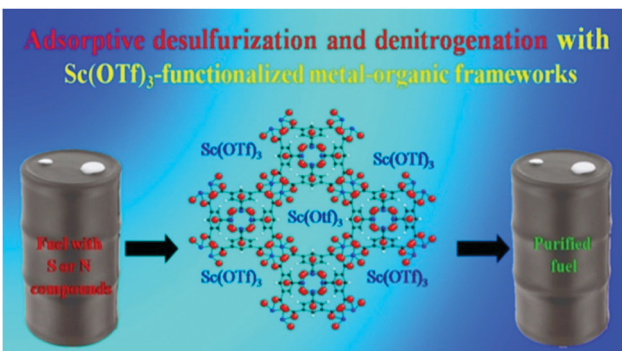


Fig. 3 Desulfurization and denitrogenation with scandium triflate MOF [reprinted with permission from ref. 61, Copyright © American Chemical Society, 2015].

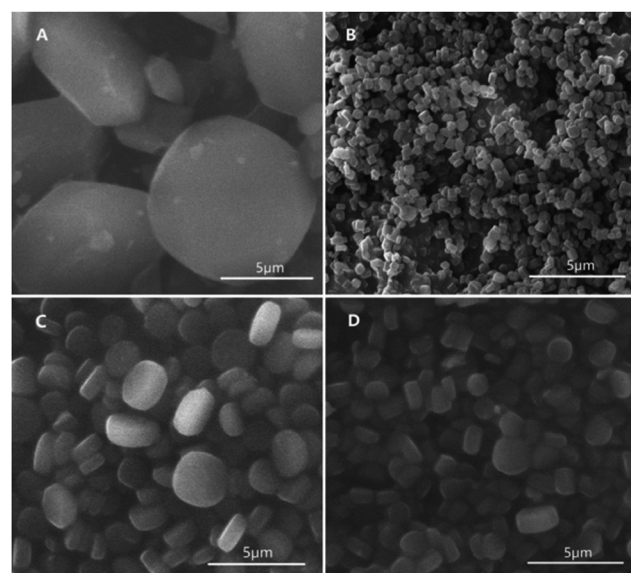


Fig. 4 SEM images of MIL-125-L (A), NH₂-MIL-125 (B), MIL-125-M (C), and MIL-125-S (D) [reprinted with permission from ref. 68, Copyright © Elsevier, 2018].



presence of methanol, both the $\text{NH}_2\text{-MIL-125}$ and MIL-125 were highly stable, and maintained the framework structure on being recycled five times.⁶⁸ Janek *et al.* synthesized tetranuclear titanium(IV) oxo-complex with 4-aminobenzoate ligands. The DFT studies were employed to confirm the formation of $[\text{Ti}_4\text{O}_2(\text{O}i\text{Bu})_{10}(\text{ABZ})_2]$ and $[\text{Ti}_6\text{O}_6(\text{O}i\text{Bu})_6(\text{ABZ})_6]$ composites. The photodegradation of methylene blue (MB) dye in UV light was investigated in the presence of Ti-MOF-complex in a polystyrene matrix.⁶⁹

A facile and scalable approach was used to fabricate porous anatase TiO_2 and $\text{Li}_4\text{Ti}_5\text{O}_{12}$ nano-tablets consisting of nanoparticles, grown from a Ti-MOF template. Both the nano-tablets exhibited outstanding electrochemical properties, and were employed as anode materials for lithium-ion batteries. TiO_2 and $\text{Li}_4\text{Ti}_5\text{O}_{12}$ delivered capacity up to 228 mA h g^{-1} and 158 mA h g^{-1} , respectively, at 0.1 A g^{-1} . The outstanding electrochemical properties were attributed to the typical porous structure which augments active sites to lodge lithium ions and enhance ionic diffusion.⁷⁰ Lian *et al.* constructed a distinct core-shell titanium-based MOF ($\text{Fe}_3\text{O}_4@\text{Cys}@\text{MIL125-NH}_2$) and applied it as a magnetic adsorbent for fluoroquinolones from aqueous samples. The developed magnetic solid phase extraction (MSPE) method showed large linear concentration range and low LOD ($0.05\text{--}0.2 \mu\text{g L}^{-1}$).⁷¹ In another work, Ti-based MOFs were synthesized by addition of tetraethyl orthosilicate. The size of synthesized Ti-based MOFs was less by 42.78% as compared to that with traditional methods. Ibuprofen (IBU) was used to investigate the controlled release property of MOFs. Approximately 95% of IBU was released from MOFs after exposure to a phosphate buffered saline system for 24 h.⁷² In another study, titanium-based MOF, MIL-125 was sulfated to increase its acidic property. The catalytic performance of raw and sulfated MIL-125 was investigated in esterification of acetic acid. It was observed that approximately 88.2% of acetic acid was converted to ester in 7 h.⁷³ Wang and co-workers synthesized titanium(IV) ion-modified COFs with outstanding performance for detection and identification of trace phospho-peptides in the complex biological samples of milk and HeLa cells.⁷⁴ It was revealed in another investigation that Ti-oxo clusters are highly selective and efficient towards photocatalysis, CO_2 reduction and pollutant degradation due to their high optical response and photo-redox properties.⁷⁵ In order to enhance the photocatalytic and degradation results, titanium-carboxylate molecular clusters and functional group tolerances of clusters were investigated by adding organic functionalities. During CO_2 cycloaddition reaction, 80% of polypropylene oxide gets converted into cyclic carbonates. The degradation studies were performed on methylene blue (MB) dye and complete degradation was achieved in 4 h.⁷⁶ George *et al.* reported microwave synthesis of titanium-based MOFs (Ti-BDC). The MOFs were observed to be photo-catalytically active (band gap energy = 3.14 eV), and effectively degraded 96.77% of MB dye in 6 h.⁷⁷ Furthermore, a hydrothermal method was used to fabricate titanium-based MOFs (porous $\text{NH}_2\text{-MIL-125}$) having high surface area ($1540 \text{ m}^2 \text{ g}^{-1}$). This MOF was successfully employed as a prospective photosensitizer and

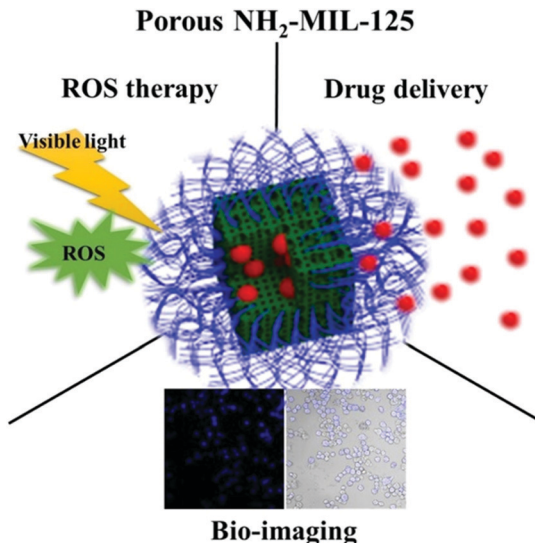


Fig. 5 Functioning of $\text{NH}_2\text{-MIL-125}$ (MOF) [reprinted with permission from ref. 78, copyright © Elsevier, 2017].

pH-responsive nano-carrier for cancer therapy, bio-imaging, drug delivery and ROS therapy (Fig. 5). Excellent results were reported during examination of breast cancer (MCF-7) cell line.⁷⁸

$\text{Fe}_3\text{O}_4@\text{SiO}_2@\text{MOF}/\text{TiO}_2$ nano-composite was prepared and utilized as an adsorbent for MSPE of tri-azole fungicides in water. The limit of detection was observed to be $0.19\text{--}1.20 \text{ ng L}^{-1}$ for the selected fungicides. This method was employed to estimate the concentration of fungicides in real life water samples.⁷⁹ Water splitting reaction and CO_2 reduction was attained with Ti doped MOFs, followed by conversion of light energy into chemical energy.⁸⁰ Guo and co-workers reported amine-functionalized MOFs ($\text{NH}_2\text{-MIL-125-Ti}$) which were used to prepare polysulfone-based mixed matrix membranes. The amalgamation of $\text{NH}_2\text{-MIL-125-Ti}$ in the membrane enhances CO_2 permeability in comparison to that of the pure polymer membrane.⁸¹

Vanadium based metal organic frameworks

The research on MOFs of vanadium is very uncommon. The clusters and complexes are formed mainly with vanadium nodes. The catalytic activity of VO_x doped $\text{MIL-101}(\text{Cr})$ was studied in gas phase ethanol oxidative dehydrogenation and it was observed that this MOF catalyst displayed excellent selectivity towards acetaldehyde (up to 99%) below 200°C .⁸² Wang and co-workers carried out the synthesis of $\text{V}/\text{UiO-66-NH}_2$ and investigated its catalytic activity for hydroxylation of benzene to phenol using O_2 . A yield of 22.0% of phenol with high selectivity (98.1%) was obtained using the fabricated MOFs in comparison to only 5.2% yield with sole UiO-66-NH_2 .⁸³ In another work, one pot *in situ* synthesis of $\text{Li}_3\text{V}_2(\text{PO}_4)_3$ /phosphorus-doped carbon (LVP/P-C) nanocomposites was carried out using hybrid vanadium MOF precursor. The nanocomposites exhibited a discharge capacity of 65 mA h g^{-1} at 10°C , and 90% of the capacity was retained after 1100 cycles.⁸⁴



Timofeev *et al.* reported isostructural metal-carboxylates MIL-100(M) and MIL-53(M) (M: V, Al, Fe and Cr) which were used in catalysis of condensation reaction of glycerol with acetone. It was observed that the materials with higher vanadium content exhibited enhanced activity and reusability at room temperature.⁸⁵ Wang *et al.* fabricated microporous MIL-47 frameworks VO (1,4-benzenedicarboxylate) with CS₂, tetrahydrothiophene, thiomorpholine and thioxane. The channel opening of framework was significantly expanded by intercalation with CS₂ by breathing deformation mode, in contrast to numerous other molecules that typically lead to contraction of channel opening. With incorporation of CS₂, maximum spherical void diameter increases to 8.0 Å from 7.6 Å of VO (1,4-benzenedicarboxylate) with empty channels.⁸⁶ The development of more stable novel materials is required as extensive leaching of active V species is observed in vanadium-based solid catalysts in liquid phase oxidation reactions. Consequently, Kim *et al.* synthesized V-based MOFs by dispersion on a carbon support, of vanadium oxide and carbide species by pyrolysis of MIL-47(V) (Fig. 6). A number of carbon catalysts containing different surface and bulk phases of V were synthesized by affecting the phase transitions of V by altering the pyrolysis temperature. Vanadium carbide catalysts displayed better performance and increased stability as confirmed by lesser amounts of V leached (<20%) in comparison to conventional V/AC (56%) during the recycling runs. This investigation signified noteworthy advancement in the development of supported V catalysts, with decreased leaching in fluid-phase oxidation reactions in contrast to materials orchestrated by ordinary impregnation strategies.⁸⁷

The electrochemical reaction of lithium with MOF, V^{IV}(O)(bdc) [MIL-47] was investigated by Kaveevivitchai *et al.* The large open

channels present in the MOF can easily lodge small ions like Li⁺. The redox properties of vanadium(IV) ions led to the use of this material as a rechargeable intercalation electrode in lithium batteries. The electrochemical properties of material were studied in Li|1 M LiPF₆ in ethylene carbonate and dimethyl carbonate V(O)(bdc) cells *vs.* Li/Li⁺ cathodes.⁸⁸ Farzaneh and Sadeghi reported a new heterogeneous catalyst Fe₃O₄@SiO₂@APTMS@VMIL-101, synthesized by incorporation of Fe₃O₄ nanoparticles modified with sodium silicate and (3-aminopropyl) trimethoxysilane (APTMS) in V-MIL-101. The epoxidation reaction of allyl alcohols and alkenes with *tert*-butyl hydroperoxide was catalysed by the material with reasonably good yield. The material was stable and reusable, thus demonstrating its heterogeneous character.⁸⁹ MOFs having open metal sites are prospective adsorbents for the separation of gaseous mixtures. Yang and co-workers investigated open-metal sites V^{III} on MIL-100V^{III/IV} and MIL-101V^{III/IV} having CO₂/CH₄/N₂/O₂ adsorption capability. It was observed that the binding energy of single O₂ on an open-metal V^{III} site is reduced to 26.5 kJ mol⁻¹ from 93.278 kJ mol⁻¹ when the sites are occupied by H₂O. XPS pattern of V 2p indicated that on removal of water coating, V-MOF changed to MIL-100V^{IV} and MIL-101V^{IV} at 25 °C owing to the effect of O₂.⁹⁰ Voort *et al.* reported V-based MOFs containing V^{III} and V^{IV} as metal nodes with their structure, porosity, stability and applications in oxidation catalysis and gas sorption.⁹¹ Two families of MOFs *i.e.* MIL-88 and MIL-101 constructed from transition metal (TM) clusters (TM = Cr, Fe, or Sc) have been recognized. Actually, these MOFs are polymorphs, fabricated from the same metal and organic linkers, but differ in the linking of components.⁹² McNamara *et al.* prepared a V-based MOF, MIL-47 and investigated its catalytic activity for oxidation of dibenzothiophene (DBT), benzothiophene,

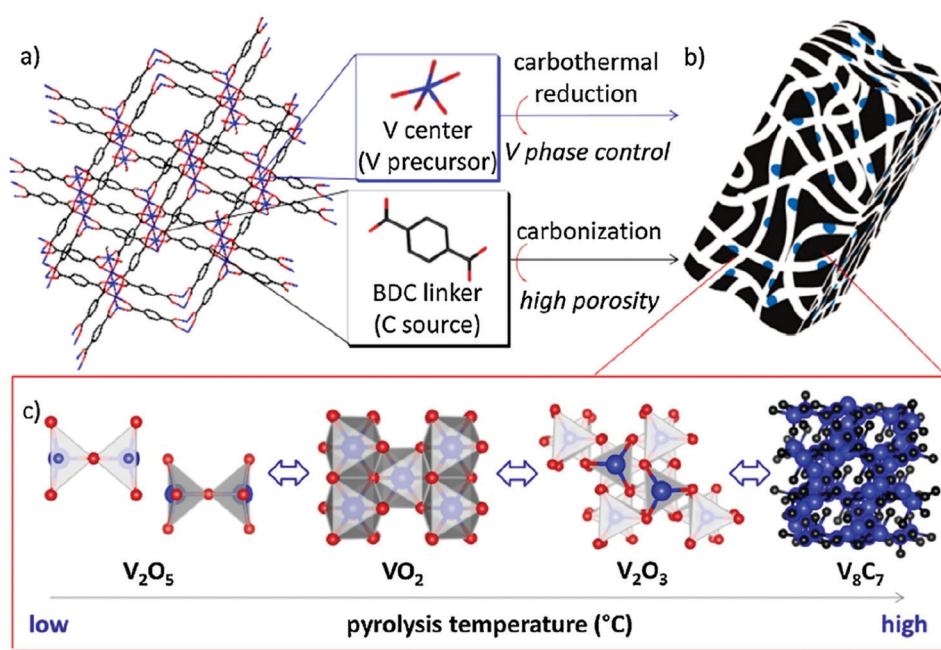


Fig. 6 Schematic representation of V-based MOFs on a carbon support via pyrolysis of MIL-47(V) [reprinted with permission from ref. 87, Copyright © Elsevier, 2016].



and thiophene. The activation energy for DBT oxidation on MIL-47 was observed to be 51 kJ mol^{-1} . It was established that better catalytic activity of MIL-47 was not merely attributed to the partial availability of active sites of MOF but also to the nature of metal centre.⁹³ The MOF, V-MIL-47, was synthesized and employed to catalyze the epoxidation of cyclohexene in different solvents. On dissolving the MOF in water, considerable leaching of V-species was observed whereas negligible leaching of the oxidant was observed on dissolution in decane. The structural framework of V-MIL-47 was retained during consecutive runs. Extensive computational modelling studies were performed to establish that a number of reaction cycles are possible.⁹⁴ Lieb *et al.* synthesized mesoporous vanadium(IV) trimesate MIL-100(V) in hydrothermal conditions. The MIL-100(V) MOF exhibited higher adsorption capability and co-ordinatively unsaturated V sites in +3 and +4 oxidation states as indicated by the *in situ* IR studies after NO exposure.⁹⁵ Rives *et al.* explored the self-diffusion of prolonged chain n-alkanes in MIL-47(V) MOF by joining quasi-elastic neutron scattering (QENS) and molecular dynamics (MD) simulations. The experimental diffusivities confirmed a non-monotonous reduction with growing chain length.⁹⁶ Phan *et al.* amalgamated homogeneous catalysts having higher activity and heterogeneous catalysts for methane activation. Vanadium based MOFs (MIL-47 & MOF-48) were observed to be chemically stable with high catalytic activity. Both the MOFs selectively transformed methane to acetic acid using $\text{K}_2\text{S}_2\text{O}_8$ as an oxidant. It was shown by isotopic labelling technique that both the methane molecules successfully transformed to acetic acid. The MOF catalysts were reusable and found to be catalytically active for a number of cycles while retaining their framework structures.⁹⁷

Chromium-based metal organic frameworks

Chromium is the fourth transition metal and first element in group six. Chromium coordinates to various organic linkers and leads to generation of different types of MOFs which are utilized for gas separation, adsorption, catalytic activity, sensing, desalination, water treatment *etc.* In catalysis, controlling the interactions between active sites and substrates is crucial. The most prominent technique is to alter the active sites with a variety of compounds which, however, reduces substrate accessibility and, as a result, diminishes activity. Thus, the construction of heterogeneous catalysts with naked metal NPs that can simultaneously modulate substrate interactions is strongly desired.⁹⁸ The surface naked metal NPs encapsulated onto MIL-101 achieved tunable interaction with the substrate and displayed outstanding catalytic activity and perfect selectivity.⁹⁹ Zhao *et al.* carried out the synthesis of MIL-101(Cr) with massive porosity, using different additives as a modifier to regulate the morphology of MOFs. The addition of NaOH yielded MOFs with high porosity and particle size of about 87 nm. The CO_2 adsorption capacity exhibited by nano-sized MIL-101(Cr) was almost twice that of bulk MIL-101(Cr).¹⁰⁰ Owing to their higher surface area and porosity, MOFs are fascinating materials for electrochemical applications,

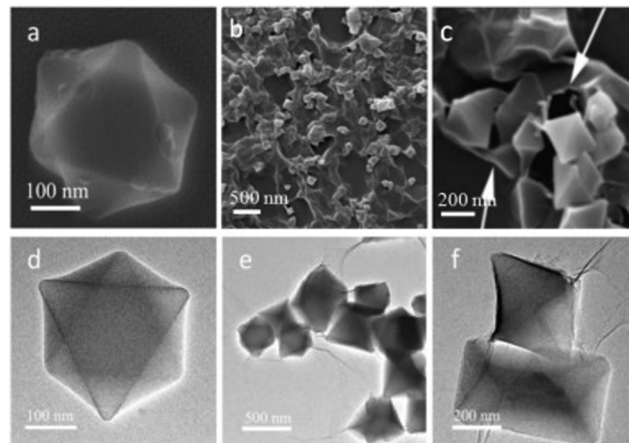


Fig. 7 (a–c) SEM and (d–f) TEM images of the MIL-101(Cr)@rGO nanocomposite [reprinted with permission from ref. 101, Copyright © Elsevier, 2018].

but poor electrical conductivity impedes their utility. Zhang and co-workers fabricated a chromium terephthalate MOF MIL-101(Cr) with reduced graphene oxide (rGO) (MIL-101(Cr)@rGO) nanocomposite (Fig. 7) which exhibited improved conductivity. The nanocomposite was employed for voltammetric monitoring of 4-nonylphenol in concentration range 0.1 to $12.5 \mu\text{M}$, with 33 nM as the detection limit.¹⁰¹

Zare *et al.* immobilized *Candida rugosa* lipase with derivatives of chromium terephthalate MIL-101(Cr) and its three improved forms: amino MIL-101(Cr) ($\text{NH}_2\text{-MIL}$), trichlorotriazine amino MIL-101(Cr) (TCT@ $\text{NH}_2\text{-MIL}$) and glutaraldehyde amino MIL-101(Cr) (Glu@ $\text{NH}_2\text{-MIL}$). The MOFs CRL@Glu@ $\text{NH}_2\text{-MIL}$ displayed highest specific activity for enzymes. Nearly 80–90% of enzyme activity was maintained after 35 days, demonstrating an outstanding storage stability of the immobilized CRLs.¹⁰² The leaking of liquid phase over the melting point and low thermal conductivity of phase change materials (PCMs) are significant hindrances that right now forestall the viable use of natural PCMs. Wang *et al.* fabricated a novel heterogeneous MOF by depositing Cr-MIL-101-NH₂ MOF nanoparticles on the surface of CNTs (Fig. 8). The combination of CNTs and MOF nanoparticles resulted in the formation of a 3D and interpenetrating network. The fabricated PEG2000/CNT/Cr-MIL-101-NH₂ composite exhibited better chemical and thermal cycling stability than PEG2000/Cr-MIL-101-NH₂ PCM.¹⁰³

Dynamic adsorption behaviour of diverse volatile organic compounds (VOCs) in gas phase on improved M-MIL-101(Cr) and MIL-101/HNO₃ was explored with special emphasis on gasoline adsorption. The growth of VOCs and measurement of their dynamic adsorption behaviour and adsorption capacity was compared on both the MOFs. Better results were obtained with MIL-101(Cr) as it adsorbed 90.14% gasoline on regeneration after 4 cycles.¹⁰⁴ Rostamnia *et al.*¹⁰⁵ synthesized open metal site MOFs of MIL-100(Cr) which were used as a support for molybdenum complexes. The $\text{MoO}(\text{O}_2)_2$ complexes were coordinated on an ethylene diamine (En)-decorated MIL-100(Cr) pore cage ($\text{MoO}(\text{O}_2)_2\text{@En/MIL-100(Cr)}$) and were successfully used for a



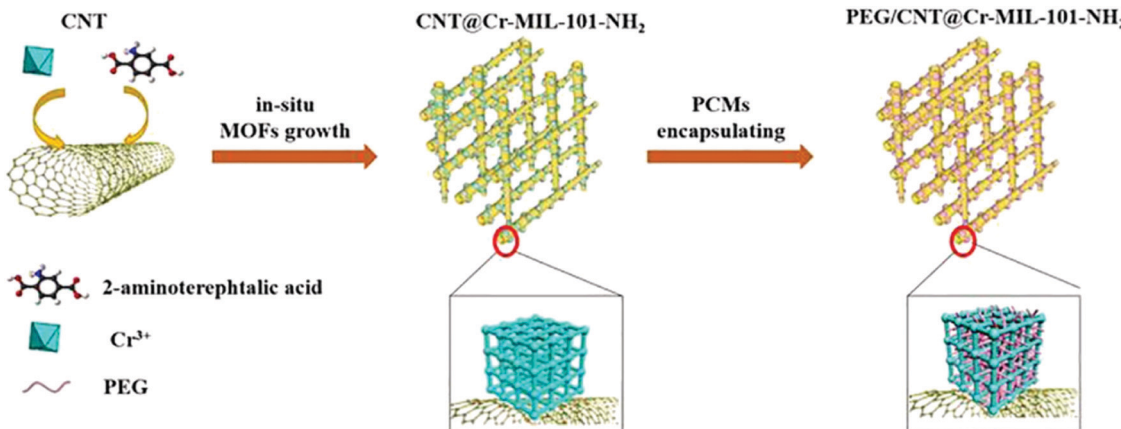


Fig. 8 Formation of the PCM composite through the CNT inserted MOFs [reprinted with permission from ref. 103, Copyright © Elsevier, 2018].

green thioether oxidation process, mediated by H_2O_2 (30%). The inimitable features like tremendously high surface area and porosity with a tuneable pore size make the MOFs an attractive material for adsorption of diverse trace pollutants from waste water. Azizi and co-workers synthesized and studied MIL-101(Cr) MOF as a proficient material for adsorption of diazinon with 92.5% removal from waste water at neutral pH. The MOFs exhibited a mesoporous octahedral structure, crystallinity and high thermal stability. The use of Langmuir isotherm for adsorption and Thomas model for system behaviour was in conformity with the results obtained.¹⁰⁶ Efficient removal of pyrethroids present in water and tea samples was achieved with the composite of MIL-101(Cr) with dispersive liquid-liquid microextraction. A linear range was achieved in concentration range 0.05–10.0 ng mL^{-1} , with sensitivity and detection limit of 0.008–0.015 ng mL^{-1} and 0.028–0.050 ng mL^{-1} , respectively. The technique was effectively employed for the estimation of pyrethroids in real life samples with acceptable recuperations.¹⁰⁷ A new approach for development of multiple adsorption sites in MIL-101(Cr) for CO_2 capture application was carried out by incorporating diethylenetriamine-based ionic liquid (DETA-Ac) by post-synthetic modification. High surface area and bulky cage size of MIL-101(Cr) led to better dispersion of ionic liquid, resulting in a higher number of sites for adsorption of CO_2 . The sole MIL-101(Cr) MOF adsorbed 1.22 mmol g^{-1} of CO_2 whereas incorporation of DETA-Ac in MIL-101(Cr) MOF increased binding sites, and 2.46 mmol g^{-1} of CO_2 was adsorbed. Cooperation of the composite and carbon dioxide resulted in high isosteric heat of adsorption.¹⁰⁸ Zhao *et al.* introduced MIL-101(Cr) MOF as an adsorbent for removing elemental mercury from sintering flue gas. Results revealed that mercury removal efficiency was increased with increase in temperature and oxygen content¹⁰⁹ (Fig. 9).

HF-free MIL-101(Cr) was synthesized hydrothermally and used for the fabrication of a highly sensitive humidity sensor with reasonably good response and recovery time. Thus, porous MIL-101(Cr) nanoparticles were established as efficient humidity sensors.¹¹⁰ The porous materials like MOFs have been widely used as adsorbents for hydrogen storage. Chromium(III) terephthalate-based MIL-101(Cr) is the most stable material among all the MOFs

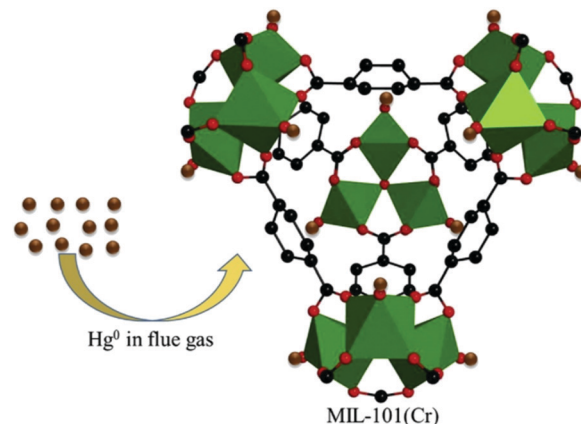


Fig. 9 Hg removal from flue gas by the open metal site of MIL-101(Cr) [reprinted with permission from ref. 109, Copyright © Elsevier, 2018].

with good uptake capacity for hydrogen. Yu *et al.* fabricated MIL-101(Cr) MOFs with huge surface area, using carbon as a surface modifier. The hybrid MOF material was employed for hydrogen storage which exhibited a capacity of 67.4 mol kg^{-1} at 77 K and 100 bar. The adsorption was measured by volumetric and gravimetric techniques.¹¹¹ Interpenetration of alkali metal ions in MIL-101(Cr) MOFs maximized the uptake of water. Iso-steric heat of adsorption was measured by the Van't Hoff equation. Doping of alkali metals (5%) resulted in a decrease of hydrophobic length and increase in water uptake, depending upon the molecular mass of metal ions.¹¹² Panchariya and co-workers prepared hybrid material of chromium(III) nitrate nonahydrate with terephthalic acid, and doping of carbon led to the fabrication of DAC/MIL-101 MOFs. Physical and chemical properties, stability and their applications were investigated to determine gas storage, adsorption and catalysis efficiency.¹¹³ Kayal *et al.* fabricated composite MAX-MIL using fluorine free hydrothermal reaction, by incorporating activated carbon *in situ* in MIL-101(Cr) MOFs. Furthermore, the adsorption of CH_4 and CO_2 on MAX-MIL and MIL-101(Cr) MOFs was compared, using gravimetric and volumetric uptakes. It was observed that the modified composite, MAX-MIL adsorbed higher amounts of CH_4 and CO_2 in comparison to the original



MIL-101(Cr) MOFs.¹¹⁴ The shape selective MIL-101(Cr) MOFs were employed as a stationary phase in gas chromatography, to separate isomers of hydrocarbons on the basis of their binding efficiency and molecular mass. Elution of linear hydrocarbons, and xylenes *i.e.* *meta*-xylene, *para*-xylene and *ortho*-xylene was studied.¹¹⁵

Catalytic adsorption of radioiodine and iodine was performed with MIL-101 in cyclohexane, and 97.9% elimination of iodine was attained. Advanced application of this reaction can be employed for controlling the amount of iodine during nuclear accidents involving radioiodine.¹¹⁶ Production of hydroxylacetone was discussed along with acetaldehyde and acetic acid from 10% oxidation of propylene glycol using tertiary butyl hydro-peroxide (TBHP) by a reaction catalysed by chromium-based MIL-101 and MIL-100 MOFs. The unsurpassed results were attained with MIL-101, employing acetonitrile as a solvent. It was observed that addition of molecular oxygen enhanced the reaction rate whereas the presence of radical chain scavengers generated a signified radical chain mechanism of oxidation process.¹¹⁷ Insertion of NH₂ in chromium based MOFs (MIL-101) was tested for enhancement of its interaction with ibuprofen and nimesulide. The liberation of ibuprofen and nimesulide was 80% and 10%, respectively, achieved in 8 days. The loading capacity of NH₂-MIL-101(Cr) is much higher in comparison to MIL-(Cr). The drugs and matrix are joined by a hydrogen bond with the help of NH₂. The release time of the drugs was extended by the matrix.¹¹⁸ Cr-MOFs were synthesised by utilization of waste PET bottles through one-pot conversion, originated from BDC acid linker. The prepared Cr-MOFs were employed for hydrogen storage applications with 1.8–2.1 wt% hydrogen uptake. Ethylene glycol and terephthalic acid were formed by depolymerisation on addition of a catalyst.¹¹⁹ Differentiation was made between MIL-101(Cr), Selexsorb CDX, Selexsorb CD, silica gel and activated carbon for the sorption of nitrogen compounds using batch and fixed-bed set ups (Fig. 10). Langmuir and Freundlich models were used for the quantification of batch test, activated carbon and MIL-101(Cr). MIL-101(Cr) retained 85–90% stability by the utilisation of acetone even after 300 cycles and exhibited 2.3 times greater adsorption efficiency than other commercial adsorbents.¹²⁰

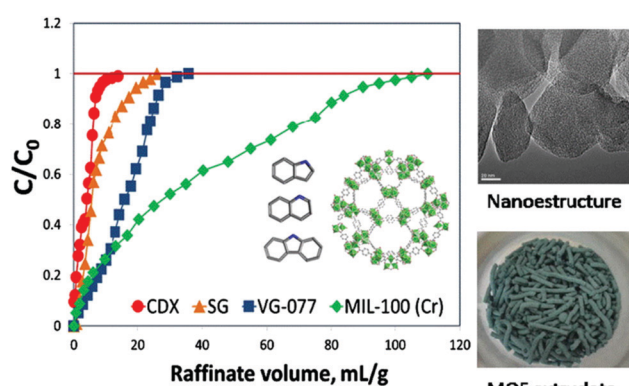


Fig. 10 Schematic representation of fabrication of MIL-100(Cr) [reprinted with permission from ref. 120, Copyright © Elsevier, 2016].

MIL-100(Fe, Cr) and MIL-101(Fe, Cr) MOFs were studied for isomerization of dicyclopentadiene from *endo* to *exo* dimers, contingent on the metal centre. MIL-100 possessed more acidic sites, high efficiency for recovery and reusability which contributed to its excellent catalytic performance.

Manganese based metal organic frameworks

Manganese is not present free in nature but is present within minerals. The ions of manganese act as co-factors for different types of enzymes. Manganese based MOFs with characteristic structural and electronic properties are fabricated mainly by a solvothermal method. Han *et al.* synthesized two new manganese based MOFs, $[\text{Mn}_2(\text{bpe})_2(4\text{-Brip})_2]_n$ (1) and $\{[\text{Mn}_3(\text{H}_2\text{O})_2(\text{H-bpp})_2(5\text{-Brip})_4]\cdot\text{H}_2\text{O}\}_n$ (2) employing a hydrothermal method. Two new polymers were isolated from aromatic poly-carboxylate and Mn(II) ions with bipyridyl ethane or bipyridyl propane ligands. Complex 1 possessed a 3D 3-fold interpenetrating network whereas complex 2 contained 1D ladder-like chains. The chains were linked by N-H···O and O-H···O hydrogen bonds to form a 2D interlocked structure.¹²¹ Owing to their large surface area, simple synthesis methods and numerous applications, MOFs are considered as highly attractive materials. Recently, MOFs have earned global recognition in the field of hydrogen storage. Hu *et al.* evaluated interrelation between hydrogen storage capacities and structure of MOFs, with reference to surface area and pore size.¹²² Zhao *et al.* synthesized $[\text{Mn}_3(\text{HCOO})_6]\text{DMF}$ MOF solvothermally, using Mn salt, formate ligand and DMF solvent. A neutral 3D network with fascinating 1D zig-zag channels was formed where the formate ligand formed a μ^3 -bridge to join three octahedral Mn(II) centers. The as-synthesized MOFs exhibited more exciting adsorption properties for CO₂ than N₂ under ambient conditions, with CO₂ uptake of 57 and 43 cm³ g⁻¹ at 273 K and 298 K, respectively.¹²³ A new hybrid material CM-MIL-101 was employed for epoxidation of alkenes and hydroxylation of alkanes using sodium periodate. The results revealed that approximately 90–95% of alkenes were converted to ketones and alcohols. Mild reaction and easy work up conditions are the unique features of this catalyst.¹²⁴

Thermal decomposition of cobalt-terephthalate and manganese MOF precursors was used for the fabrication of Mn₃O₄, Co₃O₄, and Mn₂O₃ NPs with average diameter of 60 nm, 40 nm and 80 nm, respectively. These MOFs showed great stability and reusability towards olefin oxidation. Catalytic conversion of cyclohexene yields 80–95% efficiency.¹²⁵ A 3D manganese MOF namely, $[\text{Mn}(\text{L})(\text{ndc})]_n$ was isolated using co-ligands of 2,6-naphthalenedicarboxylic acid (ndc) and 1,4-bis(5,6-dimethylbenzimidol-1-ylmethyl)benzene (L) which was employed for catalytic degradation of dye. For congo red solution, 85% degradation was attained in 130 min.¹²⁶ A series of some new Mn-MOFs was synthesized successfully under similar experimental conditions by manipulating the solvent systems. Characterization was made on the basis of XRD results showing variation in interconnections, layers of crystals and inversion center. The effect of solvents on structure



was also discussed along with the feasibility of making MOF based SBUs.¹²⁷

Iron based metal organic frameworks

Iron based MOFs having a periodic network structure are the hybrid solids formed by coordination of iron ions with organic ligands. Iron based MOFs are encouraging options in comparison to conventional heterogeneous catalysts because of their characteristic properties such as single iron sites, high porosity, and huge surface area which make available the active sites for reactants. Kailin *et al.* reported high yield conversions and better selectivity reactions within confined spaces of a micro-reactor. Furthermore, MOF catalysts were supported on the network of interconnecting channels. The huge surface area (*i.e.* 200 000 m² m⁻³) is best suited for deposition of the catalyst. ZIF-8, PdZIF-8 and FeBDC were synthesized and employed for Knoevenagel condensation reaction, selective hydrogenation reaction and acetalization reaction, respectively.¹²⁸ Presently, applications of MOFs in agriculture and food processing have started to unfold, but still the toxicity of MOFs is of great concern. MOFs based on iron carboxylate (Fe-MOFs) exhibit low toxicity and hence, can be employed in food processing in controlled doses. Abdelhameed and co-workers reported porous Fe-MOFs modified with EDTA dianhydride (Fig. 11). It was observed that Fe-MOF-EDTA exhibited better activity as compared to other Fe-sources in improving the growth rate, chlorophyll content and antioxidant enzyme activities of *Phaseolus vulgaris*.¹²⁹ The catalytic performance of iron based MOFs, namely Fe-MIL-101, Fe-MIL-100 and Fe-MIL-53 was compared for degradation of antibiotic tetracycline. It was observed that Fe-MIL-101 showed efficient removal of tetracycline (96.6%) that was much better in comparison to that of Fe-MIL-100 (57.4%) and Fe-MIL-53 (4.6%) under similar experimental conditions.

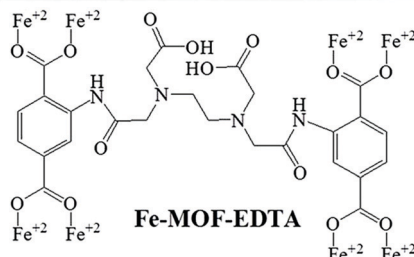


Fig. 11 Schematic representation of the fabrication of Fe-MOF-EDTA [reprinted with permission from ref. 129, Copyright © Elsevier, 2019].

It was also observed that there was significant improvement in photocatalytic degradation effect and adsorption properties with increase in time.¹³⁰ Yuan *et al.* fabricated H₂N-Fe-MIL-88B@OMC composites through *in situ* growth of H₂N-Fe-MIL-88B MOFs on ordered mesoporous carbon (OMC) by a hydrothermal method. Addition of OMC resulted in enlargement of specific surface area, lowering of electron transfer resistance, decrease of size, drastic improvement in electrochemical performance and enhancement of electro-catalytic activity for reducing *p*-nitrotoluene and oxidizing hydrazine. Hence, H₂N-Fe-MIL-88B@OMC was used for fabrication of an efficient sensor for detection of *p*-nitrotoluene and hydrazine. The sensor exhibited extensive linear range with limit of detection at 8 μM and 5.3 nM for *p*-nitrotoluene and hydrazine, respectively, under ambient conditions.¹³¹ A synthetic method for preparation of hierarchically spinel Ni_xCo_{1-x}Fe₂O₄ micro-tubes by using iron-based MOFs and inorganic acetate salts of nickel and cobalt involving combined solvent evaporation and annealing technique was used for synthesizing MOFs with adjustable sensing properties. The obtained composite exhibited high sensitivity and magnificent reproducibility for estimation of acetone vapors at 120 °C.¹³² Insertion of Cu(II) species in iron-based MOFs having large surface area reduced Cu(II) species to Cu(I). It was observed that Cu(I) doped MOFs displayed high CO/CO₂ selectivity and improved CO working ability of 1.61 mmol g⁻¹. It was also revealed that this new composite can easily separate CO/CO₂ mixtures under forceful flow conditions and can be efficiently reformed under mild conditions.¹³³ The synthesis of iron based MOFs doped with bismuth was carried out by addition of Bi(III) and MIL-101(Fe) by solvothermal method in a Teflon-lined autoclave. The new mesoporous compound exhibited enhanced uptake of iodide ions from aqueous solution. The composite displayed a fast adsorption rate that was affected by the pH of solution. During catalyst and iodide ion interactions, equilibrium was achieved in 20 min at neutral pH and 200 mg g⁻¹ concentration of iodide ions.¹³⁴ MOFs are used as heterogeneous photocatalysts, due to pores in their structures and large surface area, especially for gaseous pollutants. Pollutant gases such as nitric oxides can be oxidized by iron-based MOFs as photocatalysts. It was also observed that an iron organic framework (MIL-101) is extraordinarily stable and removed 60–70% NO_x gases under normal reaction conditions¹³⁵ (Fig. 12).

To enhance the adsorption property of iron MOFs for selenite [Se(IV)], Fe-MOFs were modified by grafting Al³⁺ ions,

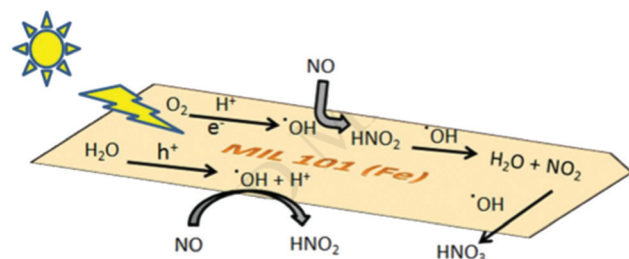


Fig. 12 Application of MOFs as a photocatalyst for the removal of pollutant gases [reprinted with permission from ref. 135, Copyright © Elsevier, 2019].



leading to Al & Fe-MOFs. Hydrolysis of Al & Fe-MOFs was carried out at pH range 3.0–7.0 which led to an increase in adsorption capacity by 77% and the efficiency of specific surface area for Se(IV) was increased by 112%, in Al@Fe-MOFs as compared to Fe-MOFs.¹³⁶ Being inexpensive and having high specific capacity, Li-S batteries have significant prospects for future energy storage. The main limitation in advancement of Li-S batteries is the low conductivity of sulfur and volume extension in the lithiation/delithiation process. High chemical adsorption among metal oxides and polysulfides encouraged the use of a $\text{Fe}_3\text{O}_4/\text{C}$ composite obtained from Fe-MOFs as a proficient sulfur host in Li-S batteries. Immobilization of sulfur and inhibition of dissipation of poly-sulfides can be carried out through the $\text{Fe}_3\text{O}_4/\text{C}$ composite due to chemical bonding between iron ions and poly-sulfides, and an interaction between oxygen anion and lithium ion. Initially, specific capacity of the battery was observed to be 1324 mA h g^{-1} at a current density of 0.05 C, and after 300 cycles, 642 mA h g^{-1} specific capacity was retained at a current density of 1.0 C. This difference and maintenance upon charging and discharging is put up on the buffer layers which are provided from the carbon component and improve the electrical conductivity as well.¹³⁷ An electrochemical biosensor based on Fe-MOFs was fabricated for signal-on detection of T4 polynucleotide kinase (PNK). Immobilization of Fe-MOFs on the electrode surface is the consequence of hybridization of Fe-MOFs & AuNPs to modify single stranded DNA to produce double stranded DNA. Electrochemical signal can be produced on the electrode surface by generation of Prussian blue through the reaction of Fe^{3+} in MOFs with $\text{K}_4\text{Fe}(\text{CN})_6$.¹³⁸ In order to produce sulfate radicals for degradation of organic contaminants, ferrocene is considered as a suitable catalyst for activating oxone. However, direct use of ferrocene in aqueous solutions may cause tough retrieval and aggregation. Ferrocene can be immobilized on some substrates without much effort. These substrates displayed small surface areas and did not offer meaningful contributions to catalytic happenings. Zhang *et al.* specifically selected a Fe-MOF, MIL-101, as a support to immobilize ferrocene chemically. The modified ferrocene-MIL (Fc-MIL) was synthesized by Schiff base reaction in which ferrocene-carboxaldehyde reacts with amine functionalized MOFs (namely, MIL-101-NH₂) (Fig. 13). Experimental studies on catalytic activity of oxone for dye degradation were taken into account. The results displayed that Fc-MIL presented higher catalytic activity and smaller activation energy.¹³⁹

Qin *et al.* established a synergistic approach to oxidize anethole selectively with H_2O_2 and *tert*-butyl hydroperoxide, using ionic liquid and Cu- or Fe-based MOFs. Nearly 95% selectivity was achieved over Cu-BTC-1 (BTC: benzene-1,3,5-tricarboxylate) with 5.0 mol% [C12mim]Cl, employing H_2O_2 as an oxidant. It was observed that the synergistic effect of Cu-BTC-1/[C12mim]Cl was responsible for enhanced reactivity.¹⁴⁰ It was reported that 2-substituted benzothiazoles can be synthesized under visible light irradiation through oxidative condensation between alcohols and o-amino thiophenols. MIL-100 and MIL-68, two iron-based MOFs were observed to be active for this reaction. Higher concentration of long-lived positive holes in MIL-68 can be photo-generated over MIL-100. Thus, MIL-100 displayed

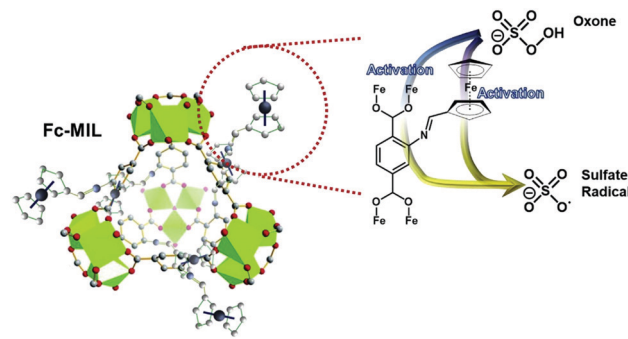


Fig. 13 Ferrocene modified MOF gives sulfate radicals and oxone on activation [reprinted with permission from ref. 139, Copyright © Elsevier, 2018].

superior catalytic performance with 92.1–94.6% selectivity and 74.8–91.5% catalytic conversion.¹⁴¹ Nikseresht and co-workers reported esterification of oleic acid with different alcohols in high yield under ultrasonic irradiation. The reaction was achieved with a heterogeneous catalyst which was invented using heteropoly acid and Fe-based MOF (MIL-53 Fe).¹⁴² Liu *et al.* developed a one-step Fe-based catalyst (Fe-MIL-88B) which exhibited better catalytic execution for converting CO_2 to hydrocarbons. At 773 K temperature, magnetite was achieved whereas the increase in temperature to 973 K resulted in metallic iron as the prominent phase. The varied performance of catalysts was due to the formation of different iron species under given reaction parameters.¹⁴³ MOFs have transformed the probable applications of nano porous materials. The most advanced applications of MOFs are their use as supports for enzyme immobilization (Fig. 14). An *in situ* approach for the synthesis of MOFs has been quite encouraging due to many reasons: (i) enzyme immobilization is achieved in a single step; (ii) it is quick; (iii) it is highly effective in encapsulation capacity; (iv) enzymes are completely engaged without any leaching; and (v) the action of engaged enzymes can be significantly preserved.¹⁴⁴

Fenton reaction is considered a proficient method for degrading highly toxic pollutants. Due to reusability and non-production of sludge, heterogeneous Fenton-like catalysts provide an encouraging substitute to homogeneous catalysts. However, these catalysts normally exhibit little activity towards production of OH because of their restricted visible active sites as well as exertion in reduction of $\text{Fe}^{(III)}$ to $\text{Fe}^{(II)}$. Hence, Cong *et al.* utilized iron-based MOFs

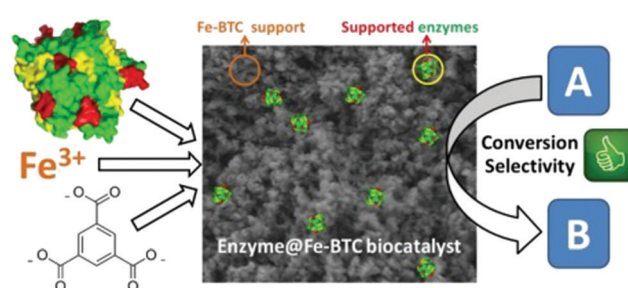


Fig. 14 Graphical representation of the synthesis of Fe-BTC MOF [reprinted with permission from ref. 144, Copyright © Elsevier, 2018].



(MIL-88-B-Fe) as a heterogeneous catalyst for degradation of pollutants. MIL-88B-Fe exhibited three times higher catalytic activity than Fe_2O_3 , $\alpha\text{-FeOOH}$, and Fe_3O_4 , traditional catalysts and MIL-53-Fe and MIL-101-Fe, the other iron-based MOFs. The combined form of MIL-88-B-Fe and H_2O_2 was capable of efficiently degrading 99% of phenol.¹⁴⁵ The adsorption capability of iron-based MOFs having square paddle-wheel cage structure for a H_2 molecule was studied. It was observed that the adsorption of H_2 molecules occurred on Fe active sites of the MOFs by interaction of d-orbitals of the MOF and sigma orbital of a H_2 molecule. The interactions were studied by DFT.¹⁴⁶ A superficial approach was established for the production of mesoporous material comprising an Fe_3O_4 core in a carbon nano disk shell employing Fe-MOF as a precursor. To affirm the presence of Fe_3O_4 nanoparticles in carbon matrix FeMCNA-300, N_2 adsorption and X-ray diffraction techniques were used. Approximately, 84% degradation of methylene blue dye was achieved in 15 min under ultra-sonication with FeMCNA-300 at the conditions of maximum iron draining.¹⁴⁷ Ehsan *et al.* fabricated Fe-based MOFs (MIL-101 Fe and MIL-88 Fe) as novel catalysts for synthesizing ethyl benzene by alkylation of benzene with ethanol. The performance of catalyst at fixed benzene to ethanol ratio at different temperatures was also observed. MIL-88 demonstrated better performance in comparison to MIL-101(Fe) for conversion of reactants (ethanol-100%, benzene-72%) and ethylbenzene selectivity (76%) at 175 °C temperature.¹⁴⁸

Due to tunability of the pore aperture and structure, MOFs are attractive materials for various applications. Araya *et al.* successfully synthesized a three-dimensional MIL-53(Fe) MOF 4 by reacting Fe-MOF with BDC linker, followed by the formation of composites with Amberlite IRA 200 and Amberlite IRA 900. The synthesized MOF composites AMIL-53(Fe) and DMIL-53(Fe) were used for degrading organic contaminants photocatalytically. By adjusting the ratio of resin to MOF, 96% of the dye was degraded in 120 min under visible light.¹⁴⁹ A crystalline Fe-based MOF-235 was fabricated and used for heterogeneous catalysis of a cyclo-condensation reaction of 1,2-diamines and ketones to form 1,5-benzodiazepines.¹⁵⁰ A study showed the immobilization application of MOFs by growth of a 3-D Fe-based MOF (MIL-100) on Fe_3O_4 compound. It resulted in the formation of a core-shell microsphere, having large surface area and magnetic characteristics, and is considered as the commendable option for enzyme immobilization. The initial activity of enzyme was >65%, and after 10 catalytic cycles, the activity was found to be 60% over 6 h. This synthesis of highly dispersed compound is an economically convenient, surfactant free and green synthesis.¹⁵¹ Anbia and co-workers synthesized iron terephthalate, MOF-235 hydrothermally that was used for gas adsorption. Among CH_4 , H_2 and CO_2 gases, maximum adsorption capacity and selectivity was shown for CH_4 . The presence of more open metal sites and large pore volume were responsible for better adsorption of CH_4 on MOF-235. The higher selectivity of MOF for CH_4 as compared to other two gases, advocated that MOF-235 was a good adsorbent for separation of CH_4 from gaseous mixtures.¹⁵² The removal of methyl orange, methylene blue or other harmful dyes from contaminated water was carried out *via* adsorption on

iron terephthalate (MOF-235). It was observed that adsorption of dyes was a spontaneous and endothermic process. Furthermore, with the adsorption of MB and MO dyes, entropy also increased.¹⁵³

Cobalt based metal organic frameworks

MOFs of cobalt display excellent applications such as adsorption, catalysis, sensing, heavy metal removal, electrical conductivity, *etc.* due to their highly crystalline and porous hybrid structure. Cobalt based MOFs can be synthesized by hydrothermal, solvothermal or wet impregnation techniques. The post-synthetic technique which allows the formation of desired structure can be used for fabrication of well-defined structural crystalline MOFs. Peters *et al.* synthesized cobalt-based MOF, NU-1000 combined with linker naphthalene dicarboxylate for blocking small cavities where cobalt oxide clusters grow (Fig. 15). For oxidative dehydrogenation of propane, cobalt oxide cluster acts as an excellent catalyst at 230 °C.¹⁵⁴

Furthermore, intensification of catalytic activity of cobalt-based MOF, Co-MOF-74@NDHPI doped with NDHPI under mild conditions was detected. The modification resulted in high selectivity of the catalyst for oxidation of toluene where molecular oxygen acted as a primary oxidant. Experimental studies showed the successful synthesis of benzoic alcohol, benzaldehyde and benzoic acid with 18%, 48% and 34% selectivity, respectively and conversion of toluene was found to be 16%.¹⁵⁵ Various electrochemical techniques were employed for insertion of titanium carbide in cobalt-based MOFs on nickel foam. The advantages of titanium carbide-based Co-MOF as the binder free supercapacitor electrode, increasing active sites and promoting fast ion transport, provide a new way for further

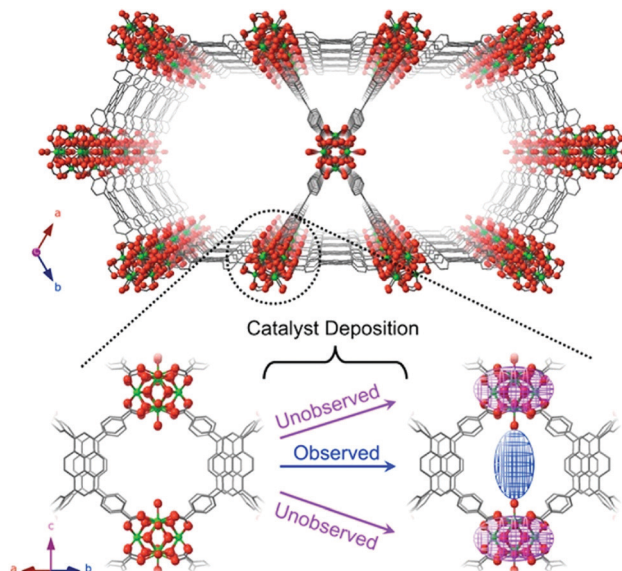


Fig. 15 Assembly of NU-1000 with stress on observed electron density of metal ions after post-synthetic anchoring of metal sites [reprinted with permission from ref. 154, Copyright © American Chemical Society, 2018].



research on such composites as it has high gravimetric capacitance.¹⁵⁶ A distinct MOF with 2-D structure was prepared by coordination of cobalt ions with bis-carboxyphenyl-triazole and bis-imidazolebenzene. On interaction with graphene, the MOF gave well organized electro-catalytic hydrogen evolution reaction (HER) with overpotential of 125 mV.¹⁵⁷ An investigation on the convenient ultrasonic technique for synthesis of cobalt terephthalate-based MOF nano-sheets having oxygen vacancies was carried out. The synthesized novel MOFs exhibited higher anodic performance that enhanced their application in sodium ion batteries. The improved working of batteries was attributed to increased ion dispersion rate and reversible sodium ion storage by the induction of electric field through oxygen vacancies.¹⁵⁸ Jiang *et al.* fabricated a single phase Co/Mn-MOF-74 composite by a hydrothermal method. The catalytic activity at low temperature was demonstrated by using it as a control catalyst for industrial NH₃-SCR NO_x degradation with 96% efficiency. Studies showed that morphology of Co/Mn-MOF-74 was affected by the incorporation of Co ions.¹⁵⁹ The MOFs are also used as outstanding electrode materials in supercapacitors. Co/Ni-MOF and Ni-MOF was fabricated hydrothermally by altering the proportion of nickel. The MOF with a dandelion like hollow structure displayed splendid specific capacitance with 75% activity retention after 5000 cycles. Experimental studies showed enhancement in electrochemical properties and improved morphology of the MOFs.¹⁶⁰ High porosity and surface area make the MOF a fascinating electrode material for energy storage and conversion. Zhu *et al.* reported a layered Co-based MOF on a nickel foam support (Co-MOF/NF) which was used as a high-performing electrode in supercapacitors. Furthermore, Co-MOF/NF demonstrated a very high specific capacitance (13.6 F cm⁻²) at 2 mA cm⁻² in 2 M KOH which was higher in comparison to other MOFs.¹⁶¹

Yu *et al.* fabricated a Co-based MOF that was carbonized and then acid etched to get mesoporous carbon, to use it as a lithium–sulfur (Li–S) battery cathode scaffold. After etching, mesoporous carbon displayed an enhancement in porosity and/or in sulfur-loading amount. In comparison to the composite-1 cathode, composite-2 (1C = 1675 mA g⁻¹) delivered a high discharge capacity of 925.1 mA h g⁻¹ in second cycle and maintained a specific value of 781.1 mA h g⁻¹ in 140th cycle.¹⁶² Enzymes, the catalysts of nature, are highly selective and efficient. In recent times, MOFs have attained great consideration as an interesting porous support for immobilizing enzymes. However, their handling and separation is still challenging, owing to less density and higher dispersion of enzyme-MOF composites. The magnetic-MOF can be a probable contender due to its advanced structural design, coupled with magnetic characteristics. Definitely fabricated magnetic-MOFs have unique properties like adjustable composition, huge surface area and speedy collection, making them a prospective candidate for immobilizing enzymes.¹⁶³ In recent years, MOFs have been considered advantageous materials for electrocatalysis. However, electrocatalytic performance and stability of synthesized MOFs was diminished by their low conductance. Murthy and co-workers prepared a cobalt hydroxide functionalized multi-walled carbon nanotube (MWCNT)

composite with improved electro activity using Co-MOF, ZIF-67 templates. The composite was used in the fabrication of a MWCNTs-Co(OH)₂ modified glassy carbon electrode (GCE) for estimation of hydrazine and hydrogen peroxide. The MWCNTs-Co(OH)₂/GCE based sensor demonstrated linear range, detection limit and sensitivity, comparable with that reported earlier for sensing of hydrazine and hydrogen peroxide.¹⁶⁴ The enhanced activity, selectivity, stability and synergic effect of dissimilar components than single component earned extensive attention. Yu *et al.* fabricated mesoporous hybrid dual-metal MOFs (Co/Fe-MOF, Fe-MOF, and Co-MOF) and studied their electrochemical properties in an ionic liquid (IL)/supercritical CO₂ (SC)/surfactant emulsion system. It was revealed that due to coexistence of two metals, Co/Fe-MOF displayed 4 times higher specific capacitance (319.5 F g⁻¹ at 1 A g⁻¹) as well as superior cycling stability compared to that of single metal Co-MOF and Fe-MOF.¹⁶⁵ In alkaline medium, electrocatalysis of glucose was performed with Co-MOF by using cobalt ions and terephthalic acid on nickel foam. Selective and sensitive examination of glucose through the production and development of non-noble metal nano-array arrangement was found to exhibit 10 886 μA mM⁻¹ cm⁻² sensitivity and 1.3 nM detection limit. The results revealed that a Co-MOF/NF compound has long-range stability and powerful reproducibility.¹⁶⁶ Owing to the ill use of antibiotics in creature farming and horticulture, it is profoundly important to estimate anti-microbials in biological systems by a straightforward, easy, and rapid strategy. Liu *et al.* fabricated a novel nano-construction, Co-MOF@TPN-COF using Co-MOF and terephthalonitrile-(TPN-COF) which was utilized as an aptasensor for sensing commonly used β-lactam antibiotic, ampicillin (AMP). The aptasensor exhibited a very low detection limit of 0.217 fg mL⁻¹ in concentration range 1.0 fg mL⁻¹–2.0 ng mL⁻¹.¹⁶⁷ The electrode property of cobalt MOF was enhanced by doping it with heteroatoms which can be further used in lithium sulfur (Li–S) batteries. By arranging the activation time and addition of a small number of clews of polymer nano belts, physiochemical properties of the doped MOFs were altered. The areal mass loading was enhanced by co-doping of the MOF defined carbon arrangement which contains cobalt and oxygen containing groups in matrix medium. This hybrid material showed transformation in activity efficiency from 1300.69 to 1020.6 mA h g⁻¹ for 0.1 and 0.5 current density after several catalytic revolutions.¹⁶⁸ The novel microporous and mesoporous cobalt-based MOF was synthesized in reduced reaction time with a simple method at low temperature. The as-synthesized lithium-ion batteries electrode displayed a high discharge capacity and respectable cyclability with a high coulombic efficiency. The micropores and mesopores of particles in materials provide sufficient space for loading and diffusion of electrolyte which is responsible for enhanced electrochemical performance.¹⁶⁹ A slow evaporation technique was used for the preparation of cobalt pyridine-dicarboxylate MOF. L-Cysteine was detected with the help of cobalt pyridine-dicarboxylate. High resistance was used for observation of signals at pH 4. The slow evaporation technique was used for preparation of $\{(C_5H_5NH)[Co(C_7H_4NO_4)(C_7H_3NO_4)] \cdot (C_7H_5NO_4) \cdot (H_2O)\}_n$ composite



bonded through covalent and non-covalent bonds.¹⁷⁰ Mehak *et al.* investigated electrochemical oxidation of methanol in an alkaline medium employing Co-MOF and its composites with GO (Co-MOF-71/GO). The composite presented exceptional peak current density (29.1 mA cm^{-2}) at lower potential (0.1 V). The boosted activity and stability was accredited to the synergy between the MOF and GO substrate.¹⁷¹ In another study, Co-MOF designed by coordination of cobalt ions with benzene-tricarboxylic acid in the presence of tri-ethylamine and nonanoic acid Co@NPC-900 displayed many advantageous properties like large surface area, proper pore sizes, highly ordered arrangement and diverse constitutions with various organic linkers, and was utilized for catalytic reaction of oxygen reduction and oxygen evolution.¹⁷² Two types of nano-crystals of Co_3O_4 were designed by indirect solid state thermolysis of cobalt terephthalate MOF (MOF-71). The MOF possessed an energy band gap of 3.7 eV and displayed outstanding stability by retaining 85% capacitance after 2000 revolutions, excellent energy density and electrochemical properties.¹⁷³ DFT calculations were performed for investigation of M-MOF-74 (M = Mg, Co or Mn). Experimental data indicated structural design, band gap energies and many other properties of MOFs. The results showed that primarily, ionic bonds and covalent bonds were observed between the metal cations and oxygen atoms. Cobalt and magnesium MOFs also possessed hydrogen bonds.¹⁷⁴ Choi *et al.* reported isostructural 3-D, Co(II) and Cd(II) MOFs using rigid 1,4-naphthalenedicarboxylate (1,4-NDC) as linkers. The 3-dimensional framework was generated by coupling of 1-dimensional chains which were formed by the bridging of metal ions with ligand. The performance of synthesized MOF as a catalyst in cyanosilylation reaction of aromatic aldehydes was investigated, and approximately 50% improved results were obtained compared to previously reported data.¹⁷⁵ The attraction for MOFs has increased owing to their probable use in high efficiency energy storage. Liu and co-workers synthesized cobalt based MOFs using tetrafluoroterephthalic acid as a linker. The MOF, with large specific capacitance and splendid cycling stability, was used as an electrode in supercapacitors (Fig. 16). The properties of Co-MOF like enough space for storage, suitable pore sizes and dispersion of electrolytes lead to its outstanding electrochemical behavior. The electrode had a specific capacitance of 2474 F g^{-1}

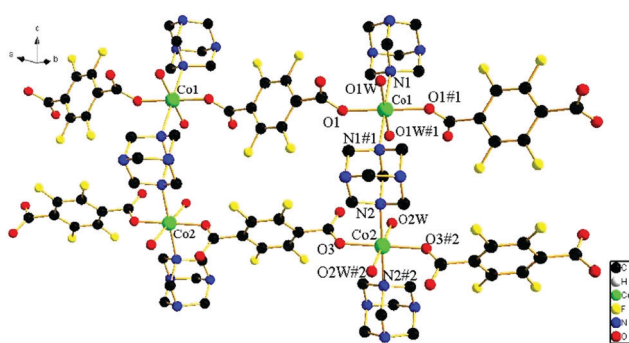


Fig. 16 2D view of Co-LMOF [reprinted with permission from ref. 176, Copyright © American Chemical Society, 2016]

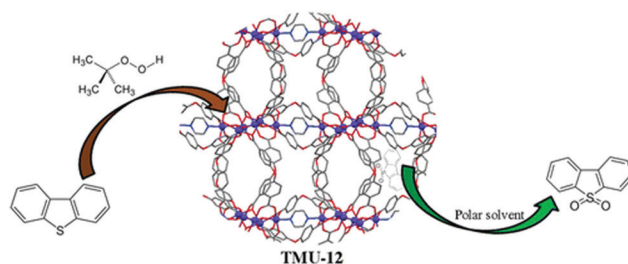


Fig. 17 Cobalt metal organic frameworks as catalysts in the oxidative desulfurization [reprinted with permission from ref. 177, Copyright © Royal Society of Chemistry, 2015].

at 1 A g^{-1} current density, and about 94.3% capacity was retained after 2000 cycles.¹⁷⁶

Co-MOF was used as a catalyst for oxidative desulfurization reaction under mild conditions (Fig. 17). Cobalt MOFs were fabricated solvothermally by the coordination of cobalt metal ions with dicarboxylate ligand. Model oil to be desulfurized, was generated by mixing dibenzothiophene in *n*-hexane. Production of the corresponding sulfone from oxidation was confirmed by FT-IR and mass analysis techniques, and 500 ppm of sulfur was removed with 75.2% efficiency in 8 h.¹⁷⁷

Trends in structural, catalytic and magnetic properties of microporous cobalt MOF, $[\text{Co}_3(\text{lac})_2(\text{pybz})_2] \cdot 3\text{DMF}$ and its derivatives prepared by ligand exchange or solvent exchange were investigated. The effect of water, DMF and other solvents on the crystal structure of MOF was studied by crystallographic technique. Upon interaction with water molecules, adsorption efficiency of Co-MOF for CH_4 , CH_3OH , C_6H_6 and I_2 gets reduced whereas post synthetic changes in structure showed transformation from antiferromagnetic to ferromagnetic.¹⁷⁸ Response of MOFs towards adsorption of gases, separation and even storage of gases in both humid and aqueous medium was studied. Almost all the MOFs are unstable in an aqueous medium whereas few such MOFs are known which show water stability. XRD, BET and N_2 adsorption studies were carried out to determine the stability of MOFs, and a useful collaboration of data was reported for advancements in MOFs.¹⁷⁹ The supercapacitor properties of cobalt MOF, synthesized from cobalt metal ion and benzene-dicarboxylate in DMF solvent, were investigated. Porous cobalt hydroxide was produced by the surface hydrolysis of Co-MOF in a basic medium. The newly formed porous cobalt hydroxide is active, and has excellent pseudo capacitance and electro-catalytic activity. Large nanoscale porosity was introduced into the products because of conformal transformation.¹⁸⁰ In current energy gadgets, efficient hydrogen evolution by electrocatalytic water splitting offers a lot of potential. Wang *et al.* reported that localized surface plasmon resonance (LSPR) excitation of Au nanorods efficiently boosted the hydrogen evolution property of CoFe-MOF nanosheets. Studies performed suggest that improved hydrogen evolution is mostly due to the injection of hot electrons from Au nanorods into CoFe-MOF nanosheets which raises the Fermi level of CoFe-MOF nanosheets, allowing for the reduction of H_2O and a lower activation energy for HER.¹⁸¹

Nickel based metal organic frameworks

Nickel is a lustrous, metallic and silver-white metal with a slight golden tinge. The enzyme of nickel like urease is used in some organisms. The MOF of Ni is formed quickly at room temperature. Arul *et al.* reported solvothermal fabrication of nickel-based MOFs capped with polyvinylpyrrolidone (Ni-MOF-PVP). Drop casting technique was used for fabrication of a GC electrode of as synthesized Ni-MOF-PVP material which was used for selective estimation of nitrobenzene (NB). It was observed that with increase in concentration (0.2 μ M–1 mM), amperometric current response of NB increased with a detection limit of 97 nM. The proposed electrode was used to determine NB in samples of tap and lake water.¹⁸² The pore size and surface structure of nickel-based MOFs can be regulated *via* a simple, cost-effective and environment friendly method by using three different molecular lengths of carboxylic acids. Large surface area and pore characteristics promote easy dispersion of electrolyte ions on the framework. Moreover, it was doped with carbon nano-fibers for increasing electrochemical performance. It exhibited high power density (1064.7 W kg⁻¹) and specific capacity (250.6 mA h g⁻¹) corresponding to 1 A g⁻¹ current density. During the catalytic process

of 5000 cycles, 92% capacity was retained.¹⁸³ Electrochemical bio-sensing application of the electro-active nickel MOFs, having large surface area and modified structural properties, was examined by Wu *et al.* Ni-MOFs were mixed with tricarboxytriphenylamine, tri-phenylamine and Ni₄O₄ for electrochemical sensing of thrombin. High selectivity and sensitivity with detection limit of 0.016 pM in the 0.05 pM–50 nM range was observed in the synthesized electro-active MOFs¹⁸⁴ (Fig. 18).

The coordination of nickel metal ion with terephthalic acid was carried out by solvothermal synthesis. The synthesized composite had a 3-D flower like structure, and its chemical stability and electrochemical activity were enhanced by ultrasonic method. A non-enzymatic electrochemical glucose sensor, with a detection limit of 4.6 μ M over a large concentration range (20 μ M–4.4 mM), was developed by the modification of Ni-MOF with a glassy carbon electrode.¹⁸⁵ The synthesis of a stable crystalline 3-D mesoporous network by coordination of a metal ion with poly-dentate organic linkers was performed through a solvothermal pathway. Nickel metal ions were coordinated with terephthalic acid using DMF solvent. X-ray studies were carried out to evaluate the crystalline nature and crystallite size. Catalytic adsorption of NO₂ with different molar ratios was studied to analyze the composition of designed MOFs. The band gap was

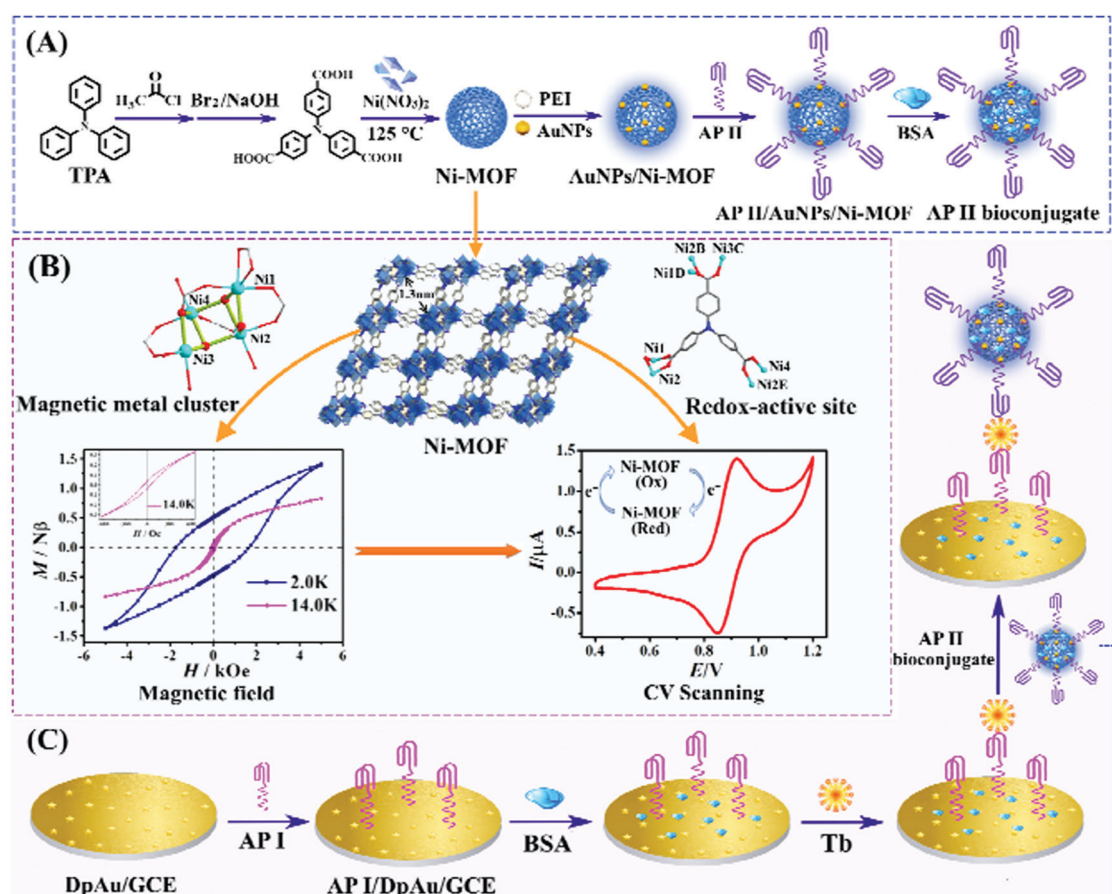


Fig. 18 Graphic demonstration of (A) preparation of AP II bioconjugate signal probe, (B) structural affected magnetic and electrochemical properties of Ni-MOF and (C) fabrication procedure of the electrochemical aptasensor for Tb detection [reprinted with permission from ref. 184, Copyright © Elsevier, 2019].



observed to be approximately 3.94 eV from UV-vis studies.¹⁸⁶ Oxidation of tetramethylbenzidine in the presence of H_2O_2 was examined with Ni-MOF. Nickel MOF is also useful for food environment analysis and in clinical medicine. In addition, a Ni-MOF nanosheet was used to design a H_2O_2 colorimetric sensor having a detection limit of 8 nM over a large concentration range (0.04–160 μM).¹⁸⁷ Hierarchical porous nickel MOF, with a perfect pore size and specific surface area was fabricated by the coordination of nickel ions with trimesic acid. By varying the concentration of trimesic acid and nickel ions, different morphologies of nickel MOFs were obtained. The studies revealed that Ni-MOF has powerful specific capacitance of 649 F g^{-1} , electrochemical properties, 63.4% rate capability and 70% retention of activity.¹⁸⁸ Microwave accelerated hydrothermal method was employed for the polymerization of coordinated 3-D MOFs of nickel metal (Ni-MOF). The experimental investigations indicated excellent surface area ($5131 \text{ m}^2 \text{ g}^{-1}$), presence of drilling open pores with radius 4.2–10.1 Å and stabilization of a 3-D structure by various hydrogen bonds (inter and intra-molecular).¹⁸⁹ The low biodegradability of industrial dye effluents makes them profoundly harmful and carcinogenic for both human and aquatic lives, and thus, they are considered unfavorable for the biodiversity of environment. Ezugwu *et al.* reported the capability of cationic Ni-MOFs for adsorbing charged and neutral dye molecules. Nickel metal ions and bis-carboxyphenyl-imidazolium chloride were used for the synthesis of cationic nickel MOF which was used for preferential elimination of methyl orange (81.08%) and congo red dyes (98.65%) by adsorption.¹⁹⁰ An investigation of the synthesis of porous Ni₂P/C composite from microwave accelerated hexagonal rods of nickel MOF was carried out. The newly prepared composite has long-term stability, highly porous arrangement, powerful electrocatalytic activity and strong electrical conductivity. The hydrogen evolution reaction (HER) was catalyzed by the electrocatalytically active Ni₂P/C composite at a potential of –64 mV and possessed capacity for long term stability.¹⁹¹ He *et al.* reported hexagonal micro-rods of MOF-74-Ni prepared with a fast and facile microwave-assisted method and applied the material as a predecessor for the generation of a porous Ni₂P/C composite. The as-synthesized Ni₂P/C displayed exceptional electrocatalytic activity for the HER. The structure of generated NiO can be optimized by varying some features of nickel MOF such as pore size, thermal behavior, specific surface area and intrinsic structural properties.¹⁹²

Synthesis of MOFs with nickel, cobalt and zinc ions, using benzene-tricarboxylic acid as a ligand, was carried out for the determination of the morphological effect on electrochemical applications and electrochemistry. XRD, FT-IR, SEM and electrochemical techniques were employed for determination of structure. Studies revealed that three MOFs have some properties similar to each other. Investigation on ponceau-4R gave the detection limit of 80 pM in 0.5–150 nM concentration range.¹⁹³ The gravimetric-type gas sensing application of Ni-MOF-74 was explored with resonant cantilever sensors in the ultrasensitive examination of carbon monoxide. Ni-MOF-74 with nanoporous structure and huge surface area holds great adsorption capacity for CO gas and it might be due to definite interaction among Ni²⁺ in Ni-MOF-74 crystal and CO molecules (Fig. 19).

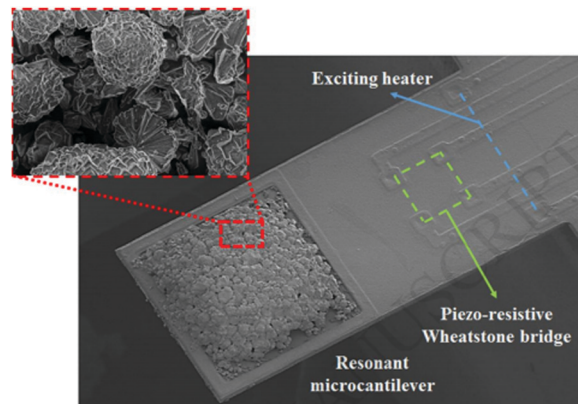


Fig. 19 MOF-loaded resonant microcantilever sensor [reprinted with permission from ref. 194, Copyright © Elsevier, 2018].

It has been observed that the gravimetric sensor developed by doping of Ni-MOF-74 on the resonant microcantilever, exhibited highly sensitive detection of CO at a trace level with less than 10 ppb (parts per billion in volume) detection limit. In addition, the sensor also exhibited outstanding reproducibility and long lasting stability.¹⁹⁴ In addition to copper or iron-based MOFs, nickel MOF has high thermal stability for the catalytic activity of NH₃-SCR. Heat treatment in N₂ atmosphere was carried out to enhance its catalytic performance and 92% of catalytic NO conversion was achieved in temperature range of 275–440 °C.¹⁹⁵ Wang *et al.* synthesized a flower-shaped MWCNTs/nickel-trimesic acid composite (MWCNTs@Ni/TA) by a solvothermal method. It was revealed that the existence of carboxyl functionalized MWCNTs helped to transform the shape of solid spherical Ni/TA. Electrochemical studies have shown that in comparison to spherical Ni(TA), flower-shaped composite achieved higher specific capacity as well as improved rate capability.¹⁹⁶ In another study, a flexible carbon cloth substrate was employed to grow Co₃O₄/Ni-based MOFs by a two-step hydrothermal method. The synthesized MOFs were employed as electrode materials and exhibited a brilliant specific capacity and good cycling stability.¹⁹⁷ The effectively peeled nanosheets from a conductive 2D-MOF Ni₃(HITP)₂ were found to be a proficient co-catalyst for CO₂ decrease in a cross breed photocatalytic framework under visible light brightening, exhibiting 97% selectivity and $3.45 \times 10^4 \mu\text{mol g}^{-1} \text{ h}^{-1}$ yield of carbon monoxide. Active sites for redox reaction and powerful conductivity for charge transfer are advantageous. This work gave fundamental insights into future structure and advancement of more powerful MOFs for CO₂ reduction.¹⁹⁸ Nickel-based Ni-MOF-74 was blended by a solvothermal strategy. Ni-MOF-74 showed excellent catalytic properties for immediate arylation of azoles by means of C–H initiation while other Ni-based MOFs, nickel-based heterogeneous frameworks, and homogeneous partners showed lower catalysis.¹⁹⁹ Tran *et al.* synthesized a Ni-MOF and MWCNTs based Ni-MOF/MWCNTs catalyst for non-enzymatic urea detection. The electrode with Ni-MOF/MWCNTs presented a tremendous sensitivity ($685 \mu\text{A mM}^{-1} \text{ cm}^{-2}$, LOD 3 μM) with 10 s response time.²⁰⁰ Qu *et al.* reported



nickel-based MOF, $[\text{Ni}(\text{L})(\text{DABCO})_{0.5}]$ where L represents a functionalized BDC (1,4-benzenedicarboxylic acid) linker and DABCO represents 1,4-diazabicyclo [2.2.2]-octane. MOF capacitors exhibited brilliant performance as electrode materials. The Ni-DMOF-ADC electrode had a specific capacitance of 552 at 1 A g⁻¹ current density and 438 F g⁻¹ at 20 A g⁻¹ current density.²⁰¹ Xu *et al.* established a superficial and effective one-step solvothermal method for the synthesis of a magnetic and porous Ni@MOF-74(Ni) $[\text{Ni}_2(\text{DOBDC})]$ $[(\text{DOBDC} = 2,5\text{-dihydroxyterephthalate})]$ composite. The as-prepared Ni@MOF-74(Ni) composite showed magnetic characteristics as well as high porosity, making the composite a competent contender for dye removal and targeted drug delivery systems. The composite displayed an adsorption capacity of 177.8 mg g⁻¹ and 4.1 mg g⁻¹ for rhodamine B and ibuprofen, respectively.²⁰² A nickel(II) pillared paddle wheel MOF was prepared *via* amalgamation of solvent-assisted linker exchange and transmetallation. The MOF showed boosted N₂ sorption performance in comparison to the isostructural Zn(II) counterpart.²⁰³ Because of their ultrahigh activity and selectivity, single-atom catalysts (SACs) are of tremendous interest. As it is challenging to make model SACs using a generic synthetic technique, distinguishing between the activity of different single-atom catalysts is difficult. Beginning from multivariate MOFs, a comprehensive technique for the production of single-atom metals implanted in N-doped carbon (M₁-N-C; M = Fe, Co, Ni, and Cu) has been established. When used in electrocatalytic CO₂ reduction, Ni₁-N-C demonstrated a very high CO faradaic efficiency (FE) of up to 96.8% which considerably outperformed other materials.²⁰⁴

Copper based metal organic frameworks

Copper is a soft and ductile metal with red orange metallic luster. Like zinc, copper is also present in trace amounts in plants and animals. MOF of copper is used in gas separation, catalysis, and super-capacitors. Cu-Based MOF can be synthesized by a solvent free method. The synthesis of novel copper-based MOFs was carried out by the addition of bioprotectant itaconic acid, and the fabricated MOF acted as an outstanding CO₂ adsorbent. The MOF was grown with dissimilar chemical formulae using diverse synthetic approaches and solvent mixtures or use of additives that may act as pore shape templating agents. On the basis of comprehensive description, Cu-IA MOF synthesized on a water-ethanol mixture reported the highest conversion and CO₂ capture.²⁰⁵ Wang *et al.* introduced Mg/Al layered double hydroxide (LDH) nanosheets as modulators for growth of HKUST-1 which is deprived of either pore blockage or loss of crystallinity (Fig. 20). The addition of LDH to HKUST-1 *via* a hydrothermal process caused phase change from octahedron (110) facets to tetrakaidecahedron (100) and (111) facets. Consequently, BET surface area and micropore volume increased significantly. HKUST-1 exhibited high acetylene uptake of 275 cm³ (STP) g⁻¹ at room temperature and 1 atm.²⁰⁶

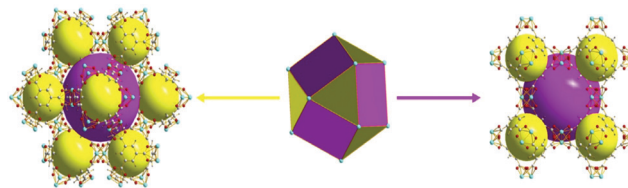


Fig. 20 Unit cells of HKUST-1 [reprinted with permission from ref. 206, Copyright © Elsevier, 2019].

Lincke *et al.* prepared and explored the crystal structure of a copper-based MOF. PXRD technique was used to confirm phase purity of the material whereas TD-PXRD and coupled DTA-TG-MS analysis confirmed its stability up to 230 °C.²⁰⁷ The catalytic property of copper-based MOF (Cu-MOF-74) was also examined. An acid catalyzed reaction of anisole was carried out for its Friedel-Crafts acylation. Effects of various parameters like temperature, acylating agent and solvent were studied on Cu-MOF. The MOF exhibited an extraordinary catalytic performance for anisole alteration and *p*-MAP yield. Furthermore, the structural MOF-74 phase was conserved when dilute acetyl chloride was used as an acylating agent.²⁰⁸ In another work, a graphene doped copper-based MOF composite was fabricated and employed for adsorption of ammonia at room temperature, under dry and moist conditions. In a dry environment, composites with lesser quantity of GO were adjudged improved adsorbents of ammonia in comparison to those having more quantity of GO. In moist environments, adsorbed ammonia caused the breakdown of MOF structure and release of active groups.²⁰⁹ The sonochemical synthesis of guanine-Cu-MOF was reported by using copper metal ions and biphenyldicarboxylic organic ligand, followed by doping of guanine. Their effect on *oprD* gene expression was determined by a broth micro-dilution method. Minimum inhibitory concentration (MIC) was observed to be 400 µg mL⁻¹, and minimum bactericidal concentration was 400 µg mL⁻¹ of *P. aeruginosa* strains.²¹⁰ Some other transition metal-based MOFs reported for various catalytic activities are listed in Table 1.

Zinc based metal organic frameworks

Zinc is a silver-grey colored compound which is present in small amounts in humans, animals, plants and microorganisms. The central nervous system is functionalized by zinc homeostasis. Zinc MOFs can be synthesized by a hydrothermal method. Sensing of compounds and adsorption of gases are major applications of zinc MOFs. Li and co-workers reported aggregation induced emission enhancement (AIEE) of AuNCs in a liquid phase *via* incarceration of AuNCs by *in situ* formed Zn-MOF. Glutathione capped AuNCs (GSH-AuNCs) were prepared by reduction of Au³⁺ by glutathione. Zn²⁺ could meaningfully improve fluorescence of GSH-AuNCs with the accumulation of 2-methylimidazole which was credited to the formation of Zn-MOF. A fluorogenic sensor was proposed for detection of Zn²⁺ in concentration range of 12.3 nM–24.6 µM, with 6 nM as the detection limit. The fabricated sensor was used for efficient estimation of zinc in human serum, milk, water,



Table 1 Some transition metal-based MOFs for different catalytic activities

Transition metal based MOFs	Method of synthesis	Morphology	Catalytic activity	Ref.
Cu-MOF	Solvothermal	Cubic	Synthesis of tacrine derivative	211
Ti-MOF	Solvothermal	Spherical	Hydrogen evolution reaction	212
Ni-MOF	Hydrothermal	Nanosheets	Hydrogen evolution reaction	213
Ni-MOF	Sonication	Stacked layers with smooth surface	Catalyst during glucose sensing	214
Mn-MOF	Solvothermal	Aggregated nanotubes	Electrode material for charge storage	215
Zr-Fu MOF	Solvothermal	Undefined shape	Adsorption of CO_2	216
Zr-Fu MOF	Solvothermal	Needle like structure	Removal of nitrates and phosphates	217
Mn-MOF	Electrochemical, solvothermal	Hexagonal rods	Adsorption of gases	218
Zn-MOF	Solvothermal	Flower like	Reduction of $\text{Cr}^{(vi)}$	219
Fe-MOF	Solvothermal	Octahedral	Reduction of N_2	220
Co-Fe MOF	Ultrasonic	Flake like	Oxygen evolution reaction	221
Co-MOF	Solvothermal	Block structure	Oxygen evolution reaction	222

and zinc sulphate syrup.²²³ Rodríguez *et al.* reported the synthesis of Zn-MOF (4,4'-bipyridyl and zinc acetate). The MOF was doped with Eu^{3+} or Tb^{3+} in different proportions. The doped Zn-MOFs exhibited characteristic red and green emission conforming to Eu^{3+} and Tb^{3+} ions, respectively. On varying the ratio of Eu^{3+} and Tb^{3+} , the color of emission by lanthanide doped Zn-MOFs changed from red to orange-yellow-green.²²⁴ Duan *et al.* reported $\{[\text{Zn}(\text{apc})_2]\text{H}_2\text{O}\}_n$ (1) and $[\text{Zn}(\text{apc})_2(\text{H}_2\text{O})_2]$ (2), with a multi-functional ligand 2-aminopyrimidine-5-carboxylic acid (Hapc). XRD investigations revealed that structure-1 consisted of an interpenetrating pillared-layer 3D framework (point symbol $\{83\}2\{86\}$), conforming to tfa topology whereas structure-2 possessed a 3D framework based on $\text{Zn}(\text{apc})_2(\text{H}_2\text{O})_2$, interlocked by hydrogen bonds.²²⁵ In another work, Zn-based MOF, $\{[(\text{CH}_3)_2\text{NH}_2]_2[\text{Zn}_5(\text{TDA})_4(\text{TZ})_4]\text{4DMF}\}_n$ (1) (H_2TDA = thiophene-2,5-dicarboxylic acid and HTZ = 1H-1,2,4-triazole) was prepared and characterized by mixed-ligand strategy. The as-synthesized material was used for detection of aniline, benzaldehyde, $\text{Cr}_2\text{O}_7^{2-}$ and CrO_4^{2-} .²⁻²²⁶ A Zn based MOF, $\{[\text{Zn}_7(\text{BPS})_4(\text{OH})_6(\text{H}_2\text{O})_2]\text{5H}_2\text{O}\}_n$, (H_2BPS = 4,4'-bibenzoic acid-2,2'-sulfone), containing wavy and infinite chain SBUs, was synthesized solvothermally. The solid-state emission spectra indicated strong luminescence emission bands at room

temperature.²²⁷ A 3D web-like carbon material C-Zn-MOF-74@CNFs was synthesized. It exhibited high electro-catalytic activity for the oxygen reduction reaction (ORR) by direct carbonization of a composite (Zn-MOF-74@CNFs) having Zn-MOF-74s grown on a carbon nano-fiber (CNF) web (Fig. 21). The solvothermal method was used to grow hexagonal pillar shaped Zn-MOF-74s with 300–600 nm diameter along with the CNF web. The calculated n value corresponding to this composite was 3.94 at 0.4 V for the ORR.²²⁸

In a study, synthesis of zinc-based MOFs through green and facile synthetic methods was discussed. The nano MOF containing biocompatible metal ions, *i.e.* zinc(II) and benzene 1,3,5-tricarboxylic acid (H_3BTC) as a linker to form $[\text{Zn}_3(\text{BTC})_2]$ using electro- and sonochemical methods was compared. The electrochemical method generated a bigger particle size (*ca.* $18.43 \pm 8.10 \mu\text{m}$) than the sonochemical method (*ca.* 87.63 ± 22.86 and 112.23 ± 28.87 nm, for 30 and 60 min, respectively). Slow-release of ibuprofen was conducted in a phosphate buffered saline system at 37°C and pH 7.4.²²⁹ Yadav *et al.* reported zinc-containing MOF-5(Zn) and MOF-5W(Zn) systems, followed by incorporation of silver which were employed in electrochemical oxidation of accumulated nitrophenols. The electrochemical and structural

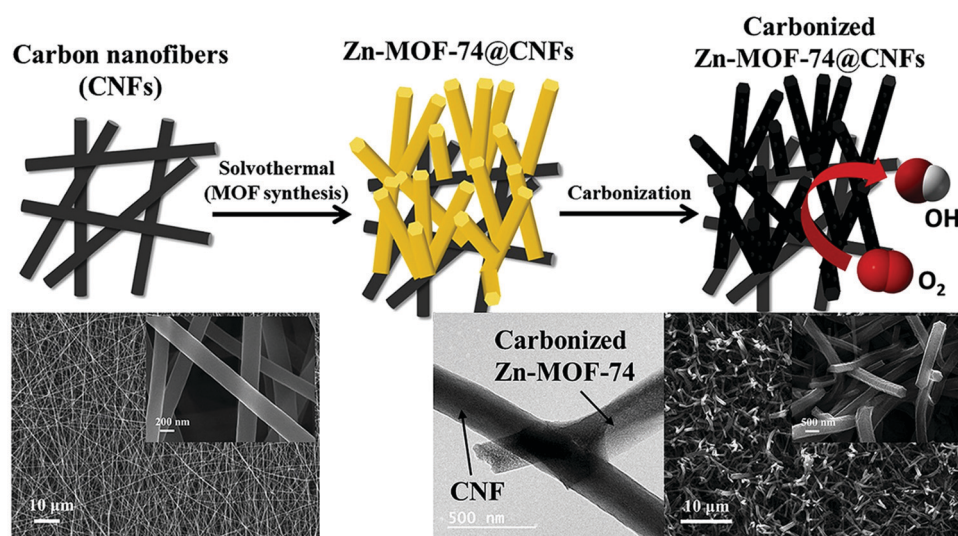


Fig. 21 Outline of the synthesis of C-Zn-MOF-74@CNFs [reprinted with permission from ref. 228, Copyright © Elsevier, 2018].



characterization revealed that silver is present in Ag@MOF-5(Zn) in metallic form. The incorporation of silver changed the electrochemical oxidation performance towards nitrophenols in MOF-5(Zn) from “inactive” to “active”.²³⁰ Wang *et al.* synthesized monodisperse MOF-5 crystals having tunable pore sizes and shapes. The synthesis comprised base-tuned nucleation and surfactant-modulated facet development of MOF-5. Under augmented reaction conditions, monodisperse MOF-5 cubes, truncated cubes, truncated octahedra, and octahedra were obtained with high reproducibility.²³¹ Mohammad *et al.* investigated adsorption of aqueous tetracycline (TC) by MOF-5, synthesized at room temperature. The MOF has cubic arrangement, 84.3% crystallinity, thermal stability up to 450 °C and about 2510 m² g⁻¹ BET surface area with both the micro- and meso-cavities. The as-synthesized material was employed for adsorptive removal of TC antibiotics, and nearly 96% of TC was removed successfully (adsorption capacity = 233 mg g⁻¹).²³² Mixed matrix membranes (MMMs) were fabricated by the introduction of MOFs, to investigate their separation properties for H₂, CO₂ and CH₄ gases. There was no direct connection between the gas adsorption capacities of MOFs and degree of permeation of these gases over the MMMs. The most adsorbed gas (H₂) infused gradually over MMMs which could be used for separation of H₂ from CO₂.^{233,234} In summary, MOFs have shown various applications such as energy storage, catalytic degradation, electrical conductivity and charge storage. The green and facile synthesis method was used for the preparation of zinc-*p*-phenylenediamine which was used for energy storage.²³⁵ The liberation of U(vi) in the atmosphere with extensive application of radionucleotides has been established. The MOF of zinc was formed by the solvothermal method, and used for the sorption of U(vi) which is spontaneous and endothermic, contingent upon pH and free from ionic strength. The researchers showed the sorption capacity (237) at pH 5 and room temperature. FTIR and XPS showed attribution to oxygen containing functional groups.²³⁶ The regulation of selectivity towards aldehydes in aromatic alcohol oxidation utilizing molecular oxygen under gentle conditions remains a major concern. Chen *et al.*²³⁷ fabricated Pt/PCN-224(M) (M = Zn, Ni, Co, Mn and 2H) composites by incorporating Pt nanocrystals and porphyrinic MOFs. Due to the strongest diamagnetism with d¹⁰ configuration of Zn²⁺ among different metals existing in a porphyrin center in the MOF, PCN-224(Zn) demonstrates the greatest ability for O₂ activation and ¹O₂ production among all the PCN-224(M) MOFs investigated.

Conclusions and future prospects

Until now, different uses of MOFs have been scrutinized as they display unique structural features, high flexibility, low cost, and high productivity. Especially on an industrial scale, MOFs illustrate promising results in waste water treatment innovations. The adaptability of structural and electronic characteristics provides the likelihood to plan materials which can be both acceptable adsorbents and effective photodegradation catalysts. Based on their large porosity, crystallinity and surface area,

MOFs are used for waste disposal, gas storage, catalytic reactions, sensing and separation procedures. Notwithstanding the turn of events and the refinements, new engineered MOFs face difficulties that come from the science of these materials and their upcoming applications. Furthermore, the possibility of extensive execution of MOFs in waste water treatment is encouraging but requires more investigation, mainly considering scaling up application to study their performance under real life conditions. Although great progress has been achieved over the past few years for fabrication of MOF materials with intrinsic catalytic activity and MOF-supported metal nanoparticles, we believe that the limitations of these systems in terms of chemical and thermal vulnerability are still a great question mark with reference to consumption. The extraordinary characteristics exhibited by MOFs have encouraged researchers to use these in numerous catalytic reactions and usually, these MOF-intervened catalysts yield better results than their conventional counterparts. However, regardless of these outstanding characteristics of MOFs, there is still a lot of opportunity to get better, and an incredible number of chemistries to be investigated. The majority of reactions over MOFs are explored for photocatalysis, electrocatalysis, thermal organic catalysis, water splitting, and the CO₂RR. Hence, extension to other catalytic procedures should be looked into by the scientific community. Also, hardly any works have reported profound examinations of the morphological changes occurring during pyrolysis. These examinations are vital as the morphology, particle size, porosity, and composition significantly rely upon the pyrolysis conditions. Thus, to highlight the change of MOFs into desired materials, *in situ* operando methods like *in situ* TEM must be achieved during pyrolysis. Finally, expansion of the MOF fabrication strategies is additionally an unquestionable requirement to get ready for the large-scale manufacturing of these promising designs. Given the outstanding characteristics of MOFs, we emphatically believe that MOFs will keep on getting broad consideration sooner rather than later, and every one of these issues will be tended to by the catalysis community.

Conflicts of interest

There are no conflicts to declare.

References

- 1 S. Qiu, M. Xue and G. Zhu, Metal-organic framework membranes: from synthesis to separation application, *Chem. Soc. Rev.*, 2014, **43**, 6116–6140.
- 2 S. Yuan, L. Feng, K. Wang, J. Pang, M. Bosch, C. Lollar, Y. Sun, J. Qin, X. Yang, P. Zhang, Q. Wang, L. Zou, Y. Zhang, L. Zhang, Y. Fang, J. Li and H. C. Zhou, Stable Metal-Organic Frameworks: Design, Synthesis, and Applications, *Adv. Mater.*, 2018, **30**, 1704303.
- 3 I. Ahmed and S. H. Jhung, Composites of metal-organic frameworks: preparation and application in adsorption, *Mater. Today*, 2014, **17**, 136–146.



4 W. Li, Metal-organic framework membranes: production, modification, and applications, *Prog. Mater. Sci.*, 2019, **100**, 21–63.

5 L. Jiao, J. Y. R. Seow, W. S. Skinner, Z. U. Wang and H. L. Jiang, Metal-organic frameworks: structures and functional applications, *Mater. Today*, 2019, **27**, 43–68.

6 S. S. Nadar, N. Varadan, O. S. Suresh, P. Rao, D. J. Ahirrao and S. Adsare, Recent progress in nanostructured magnetic framework composites (MFCs): synthesis and applications, *J. Taiwan Inst. Chem. Eng.*, 2018, **91**, 653–677.

7 N. A. Khan, Z. Hasan and S. H. Jhung, Beyond pristine metal-organic frameworks: preparation and application of nanostructured, nanosized, and analogous MOFs, *Coord. Chem. Rev.*, 2018, **376**, 20–45.

8 R. Seetharaj, P. V. Vandana, P. Arya and S. Mathew, Dependence of solvents, pH, molar ratio and temperature in tuning metal organic framework architecture, *Arab. J. Chem.*, 2019, **12**, 295–315.

9 S. K. Elsaidi, M. H. Mohamed, D. Banerjee and P. K. Thallapally, Flexibility in metal-organic frameworks: a fundamental understanding, *Coord. Chem. Rev.*, 2018, **358**, 125–152.

10 N. P. Singh and A. Kumar, Metal Organic Framework and Its Application: A Review, *Comput. Biol. Chem.*, 2016, **1**, 10–18.

11 Y. Xu, Q. Li, H. Xue and H. Pang, Metal-organic frameworks for direct electrochemical applications, *Coord. Chem. Rev.*, 2018, **376**, 292–318.

12 Y. He, F. Chen, B. Li, G. Qian, W. Zhou and B. Chen, Porous metal-organic frameworks for fuel storage, *Coord. Chem. Rev.*, 2018, **373**, 167–198.

13 B. Wang, L. H. Xie, X. Wang, X. M. Liu, J. Li and J. R. Li, Applications of metal-organic frameworks for green energy and environment: new advances in adsorptive gas separation, storage and removal, *Green Energy Environ.*, 2018, **3**, 191–228.

14 J. R. Li, J. Sculley and H. C. Zhou, Metal-Organic Frameworks for Separations, *Chem. Rev.*, 2012, **112**, 869–932.

15 Y. S. Kang, Y. Lu, K. Chen, Y. Zhao, P. Wang and W. Y. Sun, Metal-organic frameworks with catalytic centers: from synthesis to catalytic application, *Coord. Chem. Rev.*, 2019, **378**, 262–280.

16 Y. Pan, Y. Qian, X. Zheng, S. Q. Chu, Y. Yang, C. Ding, X. Wang, S. H. Yu and H. L. Jiang, Precise fabrication of single-atom alloy co-catalyst with optimal charge state for enhanced photocatalysis, *Natl. Sci. Rev.*, 2021, **8**, nwaa224.

17 Y. Wen, J. Zhang, Q. Xu, X. T. Wu and Q. L. Zhu, Pore surface engineering of metal-organic frameworks for heterogeneous catalysis, *Coord. Chem. Rev.*, 2018, **376**, 248–276.

18 L. Zhu, X. Q. Liu, H. L. Jiang and L. B. Sun, Metal-Organic Frameworks for Heterogeneous Basic Catalysis, *Chem. Rev.*, 2017, **117**, 8129–8176.

19 J. Kim, J. S. Oh, K. C. Park, G. Gupta and C. Y. Lee, Colorimetric detection of heavy metal ions in water via Metal-Organic Framework, *Inorg. Chim. Acta*, 2019, **486**, 69–73.

20 L. Wang, M. Zheng and Z. Xie, Nanoscale metal-organic frameworks for drug delivery: a conventional platform with new promise, *J. Mater. Chem. B*, 2018, **6**, 707–717.

21 A. Ma, Z. Luo, C. Gu, B. Li and J. Liu, Cytotoxicity of a metal-organic framework: drug delivery, *Inorg. Chem. Commun.*, 2017, **77**, 68–71.

22 M. Kadhom and B. Deng, Metal-organic frameworks (MOFs) in water filtration membranes for desalination and other applications, *Appl. Mater. Today*, 2018, **11**, 219–230.

23 P. Kumar, V. Bansal, K. H. Kim and E. E. Kwon, Metal-organic frameworks (MOFs) as futuristic options for wastewater treatment, *J. Ind. Eng. Chem.*, 2018, **62**, 130–145.

24 W. Du, Y. L. Bai, J. Xu, H. Zhao, L. Zhang, X. Li and J. Zhang, Advanced metal-organic frameworks (MOFs) and their derived electrode materials for supercapacitors, *J. Power Sources*, 2018, **402**, 281–295.

25 S. Sundriyal, H. Kaur, S. K. Bhardwaj, S. Mishra, K. H. Kim and A. Deep, Metal-organic frameworks and their composites as efficient electrodes for supercapacitor applications, *Coord. Chem. Rev.*, 2018, **369**, 15–38.

26 C. Vaitsis, G. Sourkouni and C. Argirousis, Metal Organic Frameworks (MOFs) and ultrasound: a review, *Ultrason. Sonochem.*, 2019, **52**, 106–119.

27 T. N. Nguyen, F. M. Ebrahim and K. C. Stylianou, Photoluminescent, upconversion luminescent and nonlinear optical metal-organic frameworks: from fundamental photophysics to potential applications, *Coord. Chem. Rev.*, 2018, **377**, 259–306.

28 K. M. Buschbaum, F. Beuerle and C. Feldmann, MOF based luminescence tuning and chemical/physical sensing, *Microporous Mesoporous Mater.*, 2015, **216**, 171–199.

29 L. Wang, Y. Han, X. Feng, J. Zhou, P. Qi and B. Wang, Metal-organic frameworks for energy storage: batteries and supercapacitors, *Coord. Chem. Rev.*, 2016, **307**, 361–381.

30 Y. Li, H. Xu, S. Ouyang and J. Ye, Metal-organic frameworks for photocatalysis, *Phys. Chem. Chem. Phys.*, 2016, **18**, 7563–7572.

31 A. Dhakshinamoorthy, A. M. Asiri and H. Garcia, Metal-organic framework (MOF) compounds: photocatalysts for redox reactions and solar fuel production, *Angew. Chem., Int. Ed.*, 2016, **55**, 5414–5445.

32 N. C. Burch, H. Jasuja and K. S. Walton, Water Stability and Adsorption in Metal-Organic Frameworks, *Chem. Rev.*, 2014, **114**, 10575–10612.

33 K. Vikrant, V. Kumar, Y. S. Ok, K. H. Kim and A. Deep, Metal-organic framework (MOF)-based advanced sensing platforms for the detection of hydrogen sulfide, *TrAC, Trends Anal. Chem.*, 2018, **105**, 263–281.

34 Y. Hu, L. Dai, D. Liu, W. Du and Y. Wang, Progress & prospect of metal-organic frameworks (MOFs) for enzyme immobilization (enzyme/MOFs), *Renewable Sustainable Energy Rev.*, 2018, **91**, 793–801.

35 P. Horcajada, R. Gref, T. Baati, P. K. Allan, G. Maurin, P. Couvreur, G. Ferey, R. E. Morris and C. Serre, Metal-Organic Frameworks in Biomedicine, *Chem. Rev.*, 2012, **112**, 1232–1268.

36 Z. Y. Gu, C. X. Yang, N. Chang and X. P. Yan, Metal-Organic Frameworks for Analytical Chemistry: From Sample Collection to Chromatographic Separation, *Acc. Chem. Res.*, 2012, **45**, 734–745.



37 A. Ayati, M. N. Shahrak, B. Tanhaei and M. Sillanpää, Emerging adsorptive removal of azo dye by metal-organic frameworks, *Chemosphere*, 2016, **160**, 30–44.

38 J. M. Yang, R. J. Ying, C. X. Han, Q. T. Hu, H. M. Xu, J. H. Li, Q. Wang and W. Zhang, Adsorptive removal of organic dyes from aqueous solution by a Zr-based metal-organic framework: effects of Ce(III) doping, *Dalton Trans.*, 2018, **47**, 3913–3920.

39 F. Rouhani, F. R. Masuleh and A. Morsali, Highly Electro-conductive Metal–Organic Framework: Tunable by Metal Ion Sorption Quantity, *J. Am. Chem. Soc.*, 2019, **141**, 11173–11182.

40 C. Petit and T. J. Bandosz, Exploring the coordination chemistry of MOF-graphite oxide composites and their applications as adsorbents, *Dalton Trans.*, 2012, **41**, 4027–4035.

41 L. R. Mingabudinova, V. V. Vinogradov, V. A. Milichko, E. Hey-Hawkins and A. V. Vinogradov, Metal–organic frameworks as competitive materials for non-linear optics, *Chem. Soc. Rev.*, 2016, **45**, 5408–5431.

42 S. Furukawa, J. Reboul, S. Diring, K. Sumida and S. Kitagawa, Structuring of metal–organic frameworks at the mesoscopic/macrosopic scale, *Chem. Soc. Rev.*, 2014, **43**, 5700–5734.

43 F. Rouhani, A. Morsali and P. Retailleau, Simple One-Pot Preparation of a Rapid Response AIE Fluorescent Metal–Organic Framework, *ACS Appl. Mater. Interfaces*, 2018, **10**(42), 36259–36266.

44 B. M. Connolly, J. P. Mehta, P. Z. Moghadam, A. E. H. Wheatley and D. Fairen-Jimenez, From synthesis to applications: metal–organic frameworks for an environmentally sustainable future, *Curr. Opin. Green Sustainable Chem.*, 2018, **12**, 47–56.

45 F. Rouhani, B. Gharib and A. Morsali, Solvent switching smart metal–organic framework as a catalyst of reduction and condensation, *Inorg. Chem. Front.*, 2019, **6**, 2412–2422.

46 M. Safaei, M. M. Foroughi, N. Ebrahimpoor, S. Jahani, A. Omedi and M. Khatami, A review on metal–organic frameworks: Synthesis and applications, *Trac, Trends Anal. Chem.*, 2019, **118**, 401–425.

47 A. Kumari, S. Kaushal and P. Singh, Bimetallic metal organic frameworks heterogeneous catalysts: design, construction, and applications, *Mater. Today Energy*, 2021, **20**, 100667.

48 B. O. Rubio, H. Ghasempour, V. Guillerm, A. Morsali, J. Juanhuix, I. Imaz and D. Maspoch, Net-Clipping: An Approach to Deduce the Topology of Metal–Organic Frameworks Built with Zigzag Ligands, *J. Am. Chem. Soc.*, 2020, **142**, 9135–9140.

49 T. F. Yi, L. J. Jiang, J. Shu, C. B. Yue, R. S. Zhu and H. B. Qiao, Recent development and application of $\text{Li}_4\text{Ti}_5\text{O}_{12}$ as anode material of lithium-ion battery, *J. Phys. Chem. Solids*, 2010, **71**(9), 1236–1242.

50 S. R. Halper, L. Do, J. R. Stork and S. M. Cohen, Topological Control in Heterometallic Metal–Organic Frameworks by Anion Templating and Metalloligand Design, *J. Am. Chem. Soc.*, 2006, **128**(47), 15255–15268.

51 Y. Wu, A. Kobayashi, G. J. Halder, V. K. Peterson, K. W. Chapman, N. Lock, P. D. Southon and C. J. Kepert, Negative Thermal Expansion in the Metal–Organic Framework Material $\text{Cu}_3(1,3,5\text{-benzenetricarboxylate})_2$, *Angew. Chem., Int. Ed.*, 2008, **47**, 8929–8932.

52 M. Klimakow, P. Klobes, K. Redemann and F. Emmerling, Characterization of mechanochemically synthesized MOFs, *Microporous Mesoporous Mater.*, 2012, **154**, 113–118.

53 N. A. Khan and S. H. Jhung, Synthesis of metal–organic frameworks (MOFs) with microwave or ultrasound: rapid reaction, phase-selectivity, and size reduction, *Coord. Chem. Rev.*, 2015, **285**, 11–23.

54 Z. Ni and R. I. Masel, Rapid Production of Metal–Organic Frameworks via Microwave-Assisted Solvothermal Synthesis, *J. Am. Chem. Soc.*, 2006, **128**, 12394–12395.

55 S. A. Razavi, M. Y. Masoomi and A. Morsali, Ultrasonic assisted synthesis of a tetrazine functionalized MOF and its application in colorimetric detection of phenylhydrazine, *Ultrason. Sonochem.*, 2017, **37**, 502–508.

56 M. O. Barsukova, S. A. Sapchenko, D. N. Dybtsev and V. P. Fedin, Scandium-organic frameworks: progress and prospects, *Russ. Chem. Rev.*, 2018, **87**(11), 1139–1167.

57 M. O. Barsukova, D. G. Samsonenko, A. A. Sapianik, S. A. Sapchenko and V. P. Fedin, Influence of synthetic conditions on the formation of thermally and hydrolytically stable Sc-based metal–organic frameworks, *Polyhedron*, 2018, **144**, 219–224.

58 L. Zhao, B. Z. Xu, J. Jia and H. S. Wu, A newly designed Sc-decorated covalent organic framework: a potential candidate for room-temperature hydrogen storage, *Comput. Mater. Sci.*, 2017, **137**, 107–112.

59 J. Cepeda, S. P. Yáñez, G. Beobide, O. Castillo, E. Goikolea, F. Aguesse, L. Garrido, A. Luque and P. A. Wright, Scandium/Alkaline Metal–Organic Frameworks: Adsorptive Properties and Ionic Conductivity, *Chem. Mater.*, 2016, **28**, 2519–2528.

60 R. S. Pillai, V. Benoit, A. Orsi, P. L. Llewellyn, P. A. Wright and G. Maurin, Highly selective CO_2 capture by small pore Scandium-based metal–organic frameworks, *J. Phys. Chem. C*, 2015, **119**, 23592–23598.

61 N. A. Khan and S. H. Jhung, Scandium-Triflate/Metal–Organic Frameworks: Remarkable adsorbents for Desulfurization and Denitrogenation, *Inorg. Chem.*, 2015, **54**, 11498–11504.

62 A. J. Graham, A. M. Banu, T. Düren, A. Greenaway, S. C. McKellar, J. P. S. Mowat, K. Ward, P. A. Wright and S. A. Moggach, Stabilization of Scandium Terephthalate MOFs against Reversible Amorphization and Structural Phase Transition by Guest Uptake at Extreme Pressure, *J. Am. Chem. Soc.*, 2014, **136**, 8606–8613.

63 C. P. Cabello, P. Rumori and G. T. Palomino, Carbon dioxide adsorption on MIL-100(M) ($M = \text{Cr}, \text{V}, \text{Sc}$) metal–organic frameworks: IR spectroscopic and thermodynamic studies, *Microporous Mesoporous Mater.*, 2014, **190**, 234–239.

64 L. Mitchell, B. Gonzalez-Santiago, J. P. S. Mowat, M. E. Gunn, P. Williamson, N. Acerbi, M. L. Clarke and P. A. Wright, Remarkable Lewis acid catalytic performance of the scandium trimesate metal organic framework MIL-100(Sc) for C–C and C≡N bond-forming reactions, *Catal. Sci. Technol.*, 2013, **3**, 606–617.



65 C. O. Areán, C. P. Cabello and G. T. Palomino, Infrared spectroscopic and thermodynamic study on hydrogen adsorption on the metal organic framework MIL-100(Sc), *Chem. Phys. Lett.*, 2012, **521**, 104–106.

66 Y. An, Y. Liu, Z. Wang, P. Wang, Z. Zheng, Y. Dai, X. Qin, X. Zhang, M. Whangbo and B. Huang, Stabilizing the titanium-based metal organic frameworks in water by metal cations with empty or partially-filled d orbitals, *J. Colloid Interface Sci.*, 2019, **533**, 9–12.

67 J. Zhu, P. Li, W. Guo, Y. Zhao and R. Zou, Titanium-based metal–organic frameworks for photocatalytic applications, *Coord. Chem. Rev.*, 2018, **359**, 80–101.

68 Y. Zhang, G. Li, L. Kong and H. Lu, Deep oxidative desulfurization catalyzed by Ti-based metal–organic frameworks, *Fuel*, 2018, **219**, 103–110.

69 M. Janek, T. M. Muziol and P. Piszczek, The structure and photocatalytic activity of the tetranuclear titanium(IV) oxo-complex with 4-aminobenzoate ligands, *Polyhedron*, 2018, **141**, 110–117.

70 J. Wang, S. Dong, Z. Yadi, Z. Chen, S. Jiang, L. Wu and X. Zhang, Metal–organic framework derived titanium-based anode materials for lithium ion batteries, *Nano-Struct. Nano-Objects*, 2018, **15**, 48–53.

71 L. Lian, X. Zhang, J. Hao, J. Lv, X. Wang, B. Zhu and D. Lou, Magnetic solid-phase extraction of fluoroquinolones from water samples using titanium-based metal–organic framework functionalized magnetic microspheres, *J. Chromatogr. A*, 2018, **1579**, 1–8.

72 Y. Xie, X. Liu, X. Ma, Y. Duan, Y. Yao and Q. Cai, Small Titanium-based MOFs prepared with the introduction of tetraethyl orthosilicate and their potential for use in drug delivery, *ACS Appl. Mater. Interfaces*, 2018, **10**, 13325–13332.

73 E. Yilmaz, E. Sert and F. S. Atalay, Synthesis and sulfation of titanium based metal organic framework; MIL-125 and usage as catalyst in esterification reactions, *Catal. Commun.*, 2017, **100**, 48–51.

74 H. Wang, F. Jiao, F. Gao, Y. Lv, Q. Wu, Y. Zhao, Y. Shen, Y. Zhang and X. Qian, Titanium(IV) ion-modified covalent organic frameworks for specific enrichment of phosphopeptides, *Talanta*, 2017, **166**, 133–140.

75 H. L. Nguyen, The chemistry of titanium-based metal–organic frameworks, *New J. Chem.*, 2017, **41**, 14030–14043.

76 S. Kim, D. Sarkar, Y. Kim, M. H. Park, M. Yoon, Y. Kim and M. Kim, Synthesis of functionalized titanium–carboxylate molecular clusters and their catalytic activity, *J. Ind. Eng. Chem.*, 2017, **53**, 171–176.

77 P. George, N. R. Dhabarde and P. Chowdhury, Rapid synthesis of Titanium based Metal Organic framework (MIL-125) via microwave route and its performance evaluation in photocatalysis, *Mater. Lett.*, 2017, **186**, 151–154.

78 A. Rengaraj, P. Puthiaraj, N. Heo, H. Lee, S. K. Hwang, S. Kwon, W. Ahn and Y. Huh, Porous NH₂-MIL-125 as an efficient nano-platform for drug delivery, imaging and ROS therapy utilised Low-Intensity Visible light exposure system, *Colloids Surf., B*, 2017, **160**, 1–10.

79 H. Su, Y. Lin, Z. Wang, Y. E. Wong, X. Chen and T. D. Chan, Magnetic metal–organic framework-titanium dioxide nanocomposite as adsorbent in the magnetic solid-phase extraction of fungicides from environmental water samples, *J. Chromatogr. A*, 2016, **1466**, 21–28.

80 R. Navarro, M. Carboni and D. Meyer, Photosensitive titanium and zirconium Metal Organic Frameworks: Current research and future possibilities, *Mater. Lett.*, 2016, **166**, 327–338.

81 X. Guo, H. Huang, Y. Ban, Q. Yang, Y. Xiao, Y. Li, W. Yang and C. Zhong, Mixed matrix membranes incorporated with amine-functionalized titanium-based metal–organic framework for CO₂/CH₄ separation, *J. Membr. Sci.*, 2015, **478**, 130–139.

82 R. Bulánek, P. Čiřmanec, J. Kotera and I. Boldog, Efficient oxidative dehydrogenation of ethanol by VO_x@MIL-101: On par with VO_x/ZrO₂ and much better than MIL-47(V), *Catal. Today*, 2019, **324**, 1–19.

83 W. Wang, N. Li, H. Tang, Y. Ma and X. Yang, Vanadium oxyacetylacetone grafted on UiO-66-NH₂ for hydroxylation of benzene to phenol with molecular oxygen, *Mol. Catal.*, 2018, **453**, 113–120.

84 Z. Wang, W. He, X. Zhang, Y. Yue, J. Liu, C. Zhang and L. Fang, Multilevel structures of Li₃V₂(PO₄)₃/phosphorous-doped carbon nanocomposites derived from hybrid V-MOFs for long-life and cheap lithium ion battery cathodes, *J. Power Sources*, 2017, **366**, 9–17.

85 M. N. Timofeeva, V. N. Panchenko, N. A. Khan, Z. Hasan, I. P. Prosvirin, S. V. Tsybulya and S. H. Jhung, Isostructural metal-carboxylates MIL-100(M) and MIL-53(M) (M: V, Al, Fe and Cr) as catalysts for condensation of glycerol with acetone, *Appl. Catal., A*, 2017, **529**, 167–174.

86 X. Wang and A. J. Jacobson, Framework deformation of the microporous vanadium benzenedicarboxylate MIL-47 upon absorption of organosulfur molecules, *Microporous Mesoporous Mater.*, 2016, **219**, 112–116.

87 J. Kim, N. D. McNamara and J. C. Hicks, Catalytic activity and stability of carbon supported V oxides and carbides synthesized via pyrolysis of MIL-47(V), *Appl. Catal., A*, 2016, **517**, 141–150.

88 W. Kaveevivitchai and A. J. Jacobson, Exploration of vanadium benzenedicarboxylate as a cathode for rechargeable lithium batteries, *J. Power Sources*, 2015, **278**, 265–273.

89 F. Farzaneh and Y. Sadeghi, Immobilized V-MIL-101 on modified Fe₃O₄ nanoparticles as heterogeneous catalyst for epoxidation of allyl alcohols and alkenes, *J. Mol. Catal. A: Chem.*, 2015, **398**, 275–281.

90 J. Yang, Y. Wang, L. Li, Z. Zhang and J. Li, Protection of open-metal V(IV) sites and their associated CO₂/CH₄/N₂/O₂/H₂O adsorption properties in mesoporous V-MOFs, *J. Colloid Interface Sci.*, 2015, **456**, 197–205.

91 P. V. D. Voort, K. Leus, Y. Liu, M. Vandichel, V. V. Speybroeck, M. Waroquier and S. Biswas, Vanadium metal–organic frameworks: structures and applications, *New J. Chem.*, 2014, **38**, 1853–1867.

92 F. Carson, J. Su, A. E. Platero-Prats, W. Wan, Y. Yun, L. Samain and X. Zou, Framework isomerism in Vanadium



Metal–Organic Frameworks: MIL-88B(V) and MIL-101(V), *Cryst. Growth Des.*, 2013, **13**, 5036–5044.

93 N. D. McNamara, G. T. Neumann, E. T. Masko, J. A. Urban and J. C. Hicks, Catalytic performance and stability of (V) MIL-47 and (Ti) MIL-125 in the oxidative desulfurization of heterocyclic aromatic sulfur compounds, *J. Catal.*, 2013, **305**, 217–226.

94 K. Leus, M. Vandichel, Y. Liu, I. Muylaert, J. Musschoot, S. Pyl, H. Vrielinck, F. Callens, G. B. Marin, C. Detavernier, P. V. Wiper, Y. Z. Khimyak, M. Waroquier, V. V. Speybroeck and P. V. D. Voort, The coordinatively saturated vanadium MIL-47 as a low leaching heterogeneous catalyst in the oxidation of cyclohexene, *J. Catal.*, 2012, **285**, 196–207.

95 A. Lieb, H. Leclerc, T. Devic, C. Serre, I. Margiakaki, F. Mahjoubi, J. S. Lee, A. Vimont, M. Daturi and J. S. Chang, MIL-100(V) – A mesoporous vanadium metal organic framework with accessible metal sites, *Microporous Mesoporous Mater.*, 2012, **157**, 18–23.

96 S. Rives, H. Jobic, F. Ragon, T. Devic, C. Serre, G. Ferey, J. Ollivier and G. Maurin, Diffusion of long chain n-alkanes in the metal–organic framework MIL-47(V): a combination of neutron scattering experiments and molecular dynamics simulations, *Microporous Mesoporous Mater.*, 2012, **164**, 259–265.

97 A. Phan, A. U. Czaja, F. Gándara, C. B. Knobler and O. M. Yaghi, Metal–Organic Frameworks of Vanadium as Catalysts for Conversion of Methane to Acetic Acid, *Inorg. Chem.*, 2011, **50**, 7388–7390.

98 L. Li, Z. Li, W. Yang, Y. Huang, G. Huang and H. L. Jiang, Integration of Pd nanoparticles with engineered pore walls in MOFs for enhanced catalysis, *Chem.*, 2021, **7**, 686–698.

99 Y. Z. Chen, B. Gu, T. Uchida, J. Liu, X. Liu, B. J. Ye, Q. Xu and H. L. Jiang, Location determination of metal nanoparticles relative to a metal–organic framework, *Nat. Commun.*, 2019, **10**, 1–10.

100 T. Zhao, S. Li, L. Shen, Y. Wang and X. Yang, The sized controlled synthesis of MIL-101(Cr) with enhanced CO₂ adsorption property, *Inorg. Chem. Commun.*, 2018, **96**, 47–51.

101 Y. Zhang, P. Yan, Q. Wan and N. Yang, Integration of chromium terephthalate metal–organic frameworks with reduced graphene oxide for voltammetry of 4-Nonylphenol, *Carbon*, 2018, **134**, 540–547.

102 A. Zare, A. Bordbar, F. Jafarian and S. Tangestaninejad, *Candida rugosa* lipase immobilization on various chemically modified Chromium terephthalate MIL-101, *J. Mol. Liq.*, 2018, **254**, 137–144.

103 J. Wang, X. Huang, H. Gao, A. Li and C. Wang, Construction of CNT@Cr-MIL-101-NH₂ hybrid composite for shape-stabilized phase change materials with enhanced thermal conductivity, *Chem. Eng. J.*, 2018, **350**, 164–172.

104 M. Shafiei, M. S. Alivand, A. Rashidi, A. Samimi and D. Mohebbi-Kalhor, Synthesis and adsorption performance of a modified micro-mesoporous MIL-101(Cr) for VOCs removal at ambient conditions, *Chem. Eng. J.*, 2018, **341**, 164–174.

105 S. Rostamnia and F. Mohsenzad, Nanoarchitecturing of open metal site Cr-MOFs for oxodiperoxo molybdenum complexes [MoO(O₂)₂@En/MIL-100(Cr)] as promising and bifunctional catalyst for selective thioether oxidation, *Mol. Catal.*, 2018, **445**, 12–20.

106 S. M. Mirsoleimani-azizi, P. Setoodeh, F. Samimi, J. Shadmehr, N. Hamedi and M. R. Rahimpour, Diazinon removal from aqueous media by mesoporous MIL-101(Cr) in a continuous fixed-bed system, *J. Environ. Chem. Eng.*, 2018, **6**, 4653–4664.

107 N. Lu, X. He, T. Wang, S. Liu and X. Hou, Magnetic solid-phase extraction using MIL-101(Cr)-based composite combined with dispersive liquid-liquid microextraction based on solidification of a floating organic droplet for the determination of pyrethroids in environmental water and tea samples, *Microchem. J.*, 2018, **137**, 449–455.

108 C. Chen, N. Feng, Q. Guo, Z. Li, X. Li, J. Ding, L. Wang, H. Wan and G. Guan, Surface engineering of a chromium metal–organic framework with bifunctional ionic liquids for selective CO₂ adsorption: synergistic effect between multiple active sites, *J. Colloid Interface Sci.*, 2018, **521**, 91–101.

109 S. Zhao, J. Mei, H. Xu, W. Liu, Z. Qu, Y. Cui and N. Yan, Research of mercury removal from sintering flue gas of iron and steel by the open metal site of MIL-101(Cr), *J. Hazard. Mater.*, 2018, **351**, 301–307.

110 J. Zhang, L. Sun, C. Chen, M. Liu, W. Dong, W. Guo and S. Ruan, High performance humidity sensor based on metal organic framework MIL-101(Cr) nanoparticles, *J. Alloys Compd.*, 2017, **695**, 520–525.

111 Z. Yu, J. Deschamps, L. Hamon, P. K. Prabhakaran and P. Pré, Hydrogen adsorption and kinetics in MIL-101(Cr) and hybrid activated carbon-MIL-101(Cr) materials, *Int. J. Hydrogen Energy*, 2017, **42**, 8021–8031.

112 H. W. B. Teo, A. Chakraborty and S. Kayal, Post synthetic modification of MIL-101(Cr) for S-shaped isotherms and fast kinetics with water adsorption, *Appl. Therm. Eng.*, 2017, **120**, 453–462.

113 D. K. Panchariya, R. K. Rai, S. K. Singh and E. A. Kumar, Synthesis and characterization of MIL-101 incorporated with Darco type Activated Charcoal, *Mater. Today*, 2017, **4**, 388–394.

114 S. Kayal and A. Chakraborty, Activated carbon (type Maxsorb-III) and MIL-101(Cr) metal organic framework based composite adsorbent for higher CH₄ storage and CO₂ capture, *Chem. Eng. J.*, 2018, **334**, 780–788.

115 H. Belarbi, L. Boudjema, C. Shepherd, N. Ramsahye, G. Toquer, J. Chang and P. Trens, Adsorption and separation of hydrocarbons by the metal organic framework MIL-101(Cr), *Colloids Surf., A*, 2017, **520**, 46–52.

116 T. Assaad and B. Assfour, Metal organic framework MIL-101 for radioiodine capture and storage, *J. Nucl. Mater.*, 2017, **493**, 6–11.

117 V. V. Torbina, I. D. Ivanchikova, O. A. Kholdeeva, I. Y. Skobelev and O. V. Vodyankina, Propylene glycol oxidation with *tert*-butyl hydroperoxide over Cr-containing metal–organic frameworks MIL-101 and MIL-100, *Catal. Today*, 2016, **278**, 97–103.

118 I. M. P. Silva, M. A. Carvalho, C. S. Oliveira, D. M. Profirio, R. B. Ferreira, P. P. Corbi and A. L. B. Formiga, Enhanced



performance of a metal-organic framework analogue to MIL-101(Cr) containing amine groups for ibuprofen and nimesulide controlled release, *Inorg. Chem. Commun.*, 2016, **70**, 47–50.

119 J. Ren, X. Dyosiba, N. M. Musyoka, H. W. Langmi, B. C. North, M. Mathe and M. S. Onyango, Green synthesis of chromium-based metal-organic framework (Cr-MOF) from waste polyethylene terephthalate (PET) bottles for hydrogen storage applications, *Int. J. Hydrogen Energ.*, 2016, **41**, 18141–18146.

120 D. Kim, H. Kim and D. Cho, Catalytic performance of MIL-100(Fe, Cr) and MIL-101(Fe, Cr) in the isomerization of endo- to exo-dicyclopentadiene, *Catal. Commun.*, 2016, **73**, 69–73.

121 M. Han, S. Li, L. Ma and L. Wang, Syntheses, structures and properties of two manganese(II) metal-organic frameworks based on bromoisophthalate and bipyridyl-type co-ligands, *Inorg. Chem. Commun.*, 2012, **20**, 340–345.

122 J. Rydén, S. Öberg, M. Heggie, M. Rayson and P. Briddon, Hydrogen storage in the manganese containing metal-organic framework MOF-73, *Microporous Mesoporous Mater.*, 2013, **165**, 205–209.

123 Y. Zhao, H. Yang, F. Wang and Z. Du, A microporous manganese-based metal-organic framework for gas sorption and separation, *J. Mol. Struct.*, 2014, **1074**, 19–21.

124 F. Zadehahmadi, S. Tangestaninejad, M. Moghadam, V. Mirkhani, I. Mohammadpoor-Baltork, A. R. Khosropour and R. Kardanpour, Manganese(III) tetracyridylporphyrin-chloromethylated MIL-101 hybrid material: a highly active catalyst for oxidation of hydrocarbons, *Appl. Catal., A*, 2014, **477**, 34–41.

125 F. Ashouri, M. Zare and M. Bagherzadeh, Manganese and cobalt-terephthalate metal-organic frameworks as a precursor for synthesis of Mn_2O_3 , Mn_3O_4 and Co_3O_4 nanoparticles: active catalysts for olefin heterogeneous oxidation, *Inorg. Chem. Commun.*, 2015, **61**, 73–76.

126 X. Wang, Y. Yu, D. Huan, K. V. Hecke and G. Cui, An unprecedented 3D manganese(II) MOF displaying (4,5)-connected xah topology, *Inorg. Chem. Commun.*, 2015, **61**, 24–26.

127 Y. Niu, L. Cui, J. Han and X. Zhao, Solvent-mediated secondary building units (SBUs) diversification in a series of MnII-based metal-organic frameworks (MOFs), *J. Solid State Chem.*, 2016, **241**, 18–25.

128 K. He, W. Han and K. L. Yeung, Preparation and performance of catalytic MOFs in microreactor, *J. Taiwan Inst. Chem. Eng.*, 2019, **98**, 85–93.

129 R. M. Abdelhameed, R. E. Abdelhameed and H. A. Kamel, Iron-based metal-organic-frameworks as fertilizers for hydroponically grown *Phaseolus vulgaris*, *Mater. Lett.*, 2019, **237**, 72–79.

130 D. Wang, F. Jia, H. Wang, F. Chen, Y. Fang, W. Dong, G. Zeng, X. Li, Q. Yang and X. Yuan, Simultaneously efficient adsorption and photocatalytic degradation of tetracycline by Fe-based MOFs, *J. Colloid Interface Sci.*, 2018, **519**, 273–284.

131 S. Yuan, X. Bo and L. Guo, *In situ* growth of iron-based metal-organic framework crystal on ordered mesoporous carbon for efficient electrocatalysis of *p*-nitrotoluene and hydrazine, *Anal. Chim. Acta*, 2018, **1024**, 73–83.

132 S. Wu, X. Li, Y. Xu, J. Wu, Z. Wang, Y. Han and X. Zhang, Hierarchical spinel $Ni_xCo_{1-x}Fe_2O_4$ microtubes derived from Fe-based MOF for high-sensitive acetone sensor, *Ceram. Int.*, 2018, **44**, 19390–19396.

133 A. Kim, T. Yoon, S. Kim, K. Cho, S. Han and Y. Bae, Creating high CO/CO₂ selectivity and large CO working capacity through facile loading of Cu(I) species into an iron-based mesoporous metal-organic framework, *Chem. Eng. J.*, 2018, **348**, 135–142.

134 W. Xu, W. Zhang, J. Kang and B. Li, Facile synthesis of mesoporous Fe-based MOFs loading bismuth with high speed adsorption of iodide from solution, *J. Solid State Chem.*, 2019, **269**, 558–565.

135 H. P. Nguyen, M. Matsuoka, T. H. Kim and S. W. Lee, Iron(III)-based metal-organic frameworks as potential visible light-driven catalysts for the removal of NO_x: a solution for urban air purification, *J. Photochem. Photobiol.*, 2018, **367**, 429–437.

136 R. Wang, H. Xu, K. Zhang, S. Wei and D. Wu, High-quality Al@Fe-MOF prepared using Fe-MOF as a micro-reactor to improve adsorption performance for selenite, *J. Hazard. Mater.*, 2019, **364**, 272–280.

137 L. Fan, H. Wu, X. Wu, M. Wang, J. Cheng, N. Zhang, Y. Feng and K. Sun, Fe-MOF derived jujube pit like Fe_3O_4/C composite as sulfur host for lithium–sulfur battery, *Electrochim. Acta*, 2019, **295**, 444–451.

138 L. Cui, J. Hu, C. Li, C. Wang and C. Zhang, An electrochemical biosensor based on the enhanced quasi-reversible redox signal of prussian blue generated by self-sacrificial label of iron metal-organic framework, *Biosens. Bioelectron.*, 2018, **122**, 168–174.

139 M. Zhang, M. Yang, S. Tong and K. A. Lin, Ferrocene-modified iron-based metal-organic frameworks as an enhanced catalyst for activating oxone to degrade pollutants in water, *Chemosphere*, 2018, **213**, 295–304.

140 H. Qin, X. Jiang, H. Huang, W. Liu, J. Li, Y. Xiao, L. Mao, Z. Fu, N. Yu and D. Yin, Ionic liquid-assisted catalytic oxidation of anethole by copper- and iron-based metal organic frameworks, *Mol. Catal.*, 2017, **440**, 158–167.

141 D. Wang, J. Albero, H. Garcia and Z. Li, Visible-light-induced tandem reaction of *o*-aminothiophenols and alcohols to benzothiazols over Fe-based MOFs: influence of the structure elucidated by transient absorption spectroscopy, *J. Catal.*, 2017, **349**, 156–162.

142 A. Nikseresht, A. Daniyal, M. Ali-Mohammadi, A. Afzalinia and A. Mirzaie, Ultrasound-assisted biodiesel production by a novel composite of Fe(III)-based MOF and phosphotungstic acid as efficient and reusable catalyst, *Ultrason. Sonochem.*, 2017, **37**, 203–207.

143 J. Liu, A. Zhang, M. Liu, S. Hu, F. Ding, C. Song and X. Guo, Fe-MOF-derived highly active catalysts for carbon dioxide hydrogenation to valuable hydrocarbons, *J. CO₂ Util.*, 2017, **21**, 100–107.



144 V. Gascon, M. B. Jimenez, R. M. Blanco and M. Sanchez-Sanchez, Semi-crystalline Fe-BTC MOF material as an efficient support for enzyme immobilization, *Catal. Today*, 2018, **304**, 119–126.

145 C. Gao, S. Chen, X. Quan, H. Yu and Y. Zhang, Enhanced Fenton-like catalysis by iron-based metal organic frameworks for degradation of organic pollutants, *J. Catal.*, 2017, **356**, 125–132.

146 M. K. Agusta, A. G. Saputro, V. V. Tanuwijaya, N. N. Hidayat and H. K. Diponoro, Hydrogen adsorption on Fe-based metal organic frameworks: DFT study, *Procedia Eng.*, 2017, **170**, 136–140.

147 M. Angamuthu, G. Satishkumar and M. V. Landau, Precisely controlled encapsulation of Fe_3O_4 nanoparticles in mesoporous carbon nanodisk using iron based MOF precursor for effective dye removal, *Microporous Mesoporous Mater.*, 2017, **251**, 58–68.

148 E. Rahmani and M. Rahmani, Alkylation of benzene over Fe-based metal organic frameworks (MOFs) at low temperature condition, *Microporous Mesoporous Mater.*, 2017, **249**, 118–127.

149 T. Araya, M. Jia, J. Yang, P. Zhao, K. Cai, W. Ma and Y. Huang, Resin modified MIL-53(Fe) MOF for improvement of photocatalytic performance, *Appl. Catal., B*, 2017, **203**, 768–777.

150 T. D. Le, K. D. Nguyen, V. T. Nguyen, T. Truong and N. T. S. Phan, 1,5-Benzodiazepine synthesis via cyclocondensation of 1,2-diamines with ketones using iron-based metal-organic framework MOF-235 as an efficient heterogeneous catalyst, *J. Catal.*, 2016, **333**, 94–101.

151 J. Wang, G. Zhao and F. Yu, Facile preparation of Fe_3O_4 @MOF core-shell microspheres for lipase immobilization, *J. Taiwan Inst. Chem. Eng.*, 2016, **69**, 139–145.

152 M. Anbia, V. Hoseini and S. Sheykhi, Sorption of methane, hydrogen and carbon dioxide on metal-organic framework, iron terephthalate (MOF-235), *J. Ind. Eng. Chem.*, 2012, **18**, 1149–1152.

153 E. Haque, J. W. Jun and S. H. Jhung, Adsorptive removal of methyl orange and methylene blue from aqueous solution with a metal-organic framework material, iron terephthalate (MOF-235), *J. Hazard. Mater.*, 2011, **185**, 507–511.

154 A. W. Peters, K. Otake, A. E. Platero-Prats, Z. Li, M. R. DeStefano, K. W. Chapman, O. K. Farha and J. T. Hupp, Site-directed synthesis of cobalt oxide clusters in a metal-organic framework, *ACS Appl. Mater. Interfaces*, 2018, **10**, 15073–15078.

155 O. Pliekhov, O. Pliekhova, U. L. Stangar and N. Z. Logar, The Co-MOF-74 modified with *N,N'*-Dihydroxypyromellitimide for selective, solvent free aerobic oxidation of toluene, *Catal. Commun.*, 2018, **110**, 88–92.

156 R. Ramachandran, K. Rajavel, W. Xuan, D. Lin and F. Wang, Influence of $\text{Ti}_3\text{C}_2\text{T}_x$ (MXene) intercalation pseudocapacitance on electrochemical performance of Co-MOF binder-free electrode, *Ceram. Int.*, 2018, **44**, 14425–14431.

157 J. Tian, M. Fu, D. Huang, X. Wang, Y. Wu, J. Y. Lu and D. Li, A new 2D Co_5 -cluster based MOF: crystal structure, magnetic properties and electrocatalytic hydrogen evolution reaction, *Inorg. Chem. Commun.*, 2018, **95**, 73–77.

158 C. Li, Q. Yang, M. Shen, J. Ma and B. Hu, The electrochemical Na intercalation/extraction mechanism of ultra-thin cobalt(II) terephthalate-based MOF nanosheets revealed by synchrotron X-ray absorption spectroscopy, *Energy Storage Mater.*, 2018, **14**, 82–89.

159 H. Jiang, Y. Niu, Q. Wang, Y. Chen and M. Zhang, Single-phase SO_2 -resistant to poisoning Co/Mn-MOF-74 catalysts for NH_3 -SCR, *Catal. Commun.*, 2018, **113**, 46–50.

160 S. Gao, Y. Sui, F. Wei, J. Qi, Q. Meng, Y. Ren and Y. He, Dandelion-like nickel/cobalt metal-organic framework based electrode materials for high performance supercapacitors, *J. Colloid Interface Sci.*, 2018, **531**, 83–90.

161 G. Zhu, H. Wen, M. Ma, W. Wang, L. Yang, L. Wang, X. Shi, X. Cheng, X. Sun and Y. Yao, A self-supported hierarchical Co-MOF as a supercapacitor electrode with ultrahigh areal capacitance and excellent rate performance, *Chem. Commun.*, 2018, **54**, 10499–10502.

162 F. Yu, H. Zhou and Q. Shen, Modification of cobalt-containing MOF-derived mesoporous carbon as an effective sulfur-loading host for rechargeable lithium-sulfur batteries, *J. Alloys Compd.*, 2019, **772**, 843–851.

163 S. S. Nadar and V. K. Rathod, Magnetic-metal organic framework (magnetic-MOF): a novel platform for enzyme immobilization and nanozyme applications, *Int. J. Biol. Macromol.*, 2018, **120**, 2293–2302.

164 N. M. Umesh, K. K. Rani, R. Devasenathipathy, B. Sriram, Y. Liu and S. Wang, Preparation of Co-MOF derived $\text{Co}(\text{OH})_2$ /multiwalled carbon nanotubes as an efficient bifunctional electro catalyst for hydrazine and hydrogen peroxide detections, *J. Taiwan Inst. Chem. Eng.*, 2018, **93**, 79–86.

165 H. Yu, H. Xia, J. Zhang, J. He, S. Guo and Q. Xu, Fabrication of Fe-doped Co-MOF with mesoporous structure for the optimization of supercapacitor performances, *Chin. Chem. Lett.*, 2018, **29**, 834–836.

166 Y. Li, M. Xie, X. Zhang, Q. Liu, D. Lin, C. Xu, F. Xie and X. Sun, Co-MOF nanosheet array: a high-performance electrochemical sensor for non-enzymatic glucose detection, *Sens. Actuators, B*, 2019, **278**, 126–132.

167 X. Liu, M. Hu, M. Wang, Y. Song, N. Zhou, L. He and Z. Zhang, Novel nanoarchitecture of Co-MOF-on-TPN-COF hybrid: ultralowly sensitive bioplatform of electrochemical aptasensor toward ampicillin, *Biosens. Bioelectron.*, 2019, **123**, 59–68.

168 W. Jin, J. Zou, S. Zeng, S. Inguva, G. Xu, X. Li, M. Peng and X. Zeng, Tailoring the structure of clew-like carbon skeleton with 2D Co-MOF for advanced Li-S cells, *Appl. Surf. Sci.*, 2019, **469**, 404–413.

169 P. Sengodu, C. Bongu, M. Perumal and M. Paramasivam, Easy synthesis of microporous/mesoporous cobalt organic framework as binder less lithium-ion battery electrode, *J. Alloys Compd.*, 2017, **714**, 603–609.

170 T. W. Murinzi, E. Hosten and G. M. Watkins, Synthesis and characterization of a cobalt-2,6-pyridinedicarboxylate MOF



with potential application in electrochemical sensing, *Polyhedron*, 2017, **137**, 188–196.

171 R. Mehek, N. Iqbal, T. Noor, H. Nasir, Y. Mehmood and S. Ahmed, Novel Co-MOF/Graphene Oxide electrocatalyst for methanol oxidation, *Electrochim. Acta*, 2017, **255**, 195–204.

172 H. Lu, H. Zhang, R. Liu, X. Zhang, H. Zhao and G. Wang, Macroscale cobalt-MOFs derived metallic Co nanoparticles embedded in N-doped porous carbon layers as efficient oxygen electrocatalysts, *Appl. Surf. Sci.*, 2017, **392**, 402–409.

173 H. Bigdeli, M. Moradi, S. Hajati, M. A. Kiani and J. Toth, Cobalt terephthalate MOF-templated synthesis of porous nano-crystalline Co_3O_4 by the new indirect solid state thermolysis as cathode material of asymmetric supercapacitor, *Phys. E*, 2017, **94**, 158–166.

174 A. D. Oliveira, G. F. D. Lima and H. A. D. Abreu, Structural and electronic properties of M-MOF-74 (M = Mg, Co or Mn), *Chem. Phys. Lett.*, 2018, **691**, 283–290.

175 I. Choi, Y. Kim, D. N. Lee and S. Huh, Three-dimensional cobalt(II) and cadmium(II) MOFs containing 1,4-naphthalene-dicarboxylate: catalytic activity of Cd-MOF, *Polyhedron*, 2016, **105**, 96–103.

176 X. Liu, C. Shi, C. Zhai, M. Cheng, Q. Liu and G. Wang, Cobalt-based layered metal-organic framework as an ultra-high capacity supercapacitor electrode material, *ACS Appl. Mater. Interfaces*, 2016, **8**, 4585–4591.

177 M. Y. Masoomi, M. Bagheri and A. Morsali, Application of two cobalt-based metal-organic frameworks as oxidative desulfurization catalysts, *Inorg. Chem.*, 2015, **54**, 11269–11275.

178 M. Zeng, Z. Yin, Y. Tan, W. Zhang, Y. He and M. Kurmoo, Nanoporous cobalt(II) MOF exhibiting four magnetic ground states and changes in gas sorption upon post-synthetic modification, *J. Am. Chem. Soc.*, 2014, **136**, 4680–4688.

179 H. Jasuja, Y. Jiao, N. C. Burtch, Y. G. Huang and K. S. Walton, Synthesis of Cobalt-, Nickel-, Copper-, and Zinc-based, Water-stable, Pillared Metal-Organic Frameworks, *Langmuir*, 2014, **30**, 14300–14307.

180 D. O. Miles, D. Jiang, A. D. Burrows, J. E. Halls and F. Marken, Conformal transformation of $[\text{Co}(\text{bdc})(\text{DMF})]$ (Co-MOF-71, bdc = 1,4-benzenedicarboxylate, DMF = *N,N*-dimethylformamide) into porous electrochemically active cobalt hydroxide, *Electrochim. Commun.*, 2013, **27**, 9–13.

181 S. S. Wang, L. Jiao, Y. Qian, W. C. Hu, G. Y. Xu, C. Wang and H. L. Jiang, Boosting Electrocatalytic Hydrogen Evolution over Metal-Organic Frameworks by Plasmon-Induced Hot-Electron Injection, *Angew. Chem., Int. Ed.*, 2019, **58**, 10713–10717.

182 P. Arul and S. A. John, Size controlled synthesis of Ni-MOF using polyvinylpyrrolidone: new electrode material for the trace level determination of nitrobenzene, *J. Electroanal. Chem.*, 2018, **829**, 168–176.

183 C. R. Rawool, S. P. Karna and A. K. Srivastava, Enhancing the supercapacitive performance of Nickel based metal organic framework-carbon nanofibers composite by changing the ligands, *Electrochim. Acta*, 2019, **294**, 345–356.

184 H. Wu, M. Li, Z. Wang, H. Yu, J. Han, G. Xie and S. Chen, Highly stable Ni-MOF comprising triphenylamine moieties as a high-performance redox indicator for sensitive apta-sensor construction, *Anal. Chim. Acta*, 2019, **1049**, 74–81.

185 F. Wang, X. Chen, L. Chen, J. Yang and Q. Wang, High-performance non-enzymatic glucose sensor by hierarchical flower-like nickel(II)-based MOF/carbon nanotubes composite, *Mater. Sci. Eng., C*, 2019, **96**, 41–50.

186 A. Katoch, R. Bhardwaj, N. Goyal and S. Gautam, Synthesis, structural and optical study of Ni-doped Metal-organic framework for adsorption based chemical sensor application, *Vacuum*, 2018, **158**, 249–256.

187 J. Chen, Y. Shu, H. Li, Q. Xu and X. Hu, Nickel metal-organic framework 2D nanosheets with enhanced peroxidase nanzyme activity for colorimetric detection of H_2O_2 , *Talanta*, 2018, **189**, 254–261.

188 P. Du, Y. Dong, C. Liu, W. Wei, D. Liu and P. Liu, Fabrication of hierarchical porous nickel based metal-organic framework (Ni-MOF) constructed with nanosheets as novel pseudocapacitive material for asymmetric supercapacitor, *J. Colloid Interface Sci.*, 2018, **518**, 57–68.

189 K. M. Elsabawy and A. M. Fallatah, Microwave assisted synthesis and molecular structure visualization of ultra-high surface area Ni-6,6'-dibromo-indigo coordinated polymeric MOFs stabilized via hydrogen bonding, *Inorg. Chem. Commun.*, 2018, **92**, 78–83.

190 C. I. Ezugwu, M. A. Asraf, X. Li, S. Liu, C. Kao, S. Zhuiykov and F. Verpoort, Cationic Nickel Metal-organic frameworks for adsorption of negatively charged dye molecules, *Data Brief*, 2018, **18**, 1952–1961.

191 S. He, S. He, X. Bo, Q. Wang, F. Zhan, Q. Wang and C. Zhao, Porous $\text{Ni}_2\text{P}/\text{C}$ microrods derived from microwave-prepared MOF-74-Ni and its electrocatalysis for hydrogen evolution reaction, *Mater. Lett.*, 2018, **231**, 94–97.

192 X. Hou, X. Yan, X. Wang and Q. Zhai, Tuning the porosity of mesoporous NiO through calcining isostructural Ni-MOFs toward supercapacitor applications, *J. Solid State Chem.*, 2018, **263**, 72–78.

193 L. Ji, Y. Jin, K. Wu, C. Wan, N. Yang and Y. Tang, Morphology-dependent electrochemical sensing performance of metal (Ni, Co, Zn)-organic frameworks, *Anal. Chim. Acta*, 2018, **1031**, 60–66.

194 Y. Lv, P. Xu, H. Yu, J. Xu and X. Li, Ni-MOF-74 as Sensing Material for Resonant-gravimetric Detection of ppb-level CO, *Sens. Actuators, B*, 2018, **262**, 562–569.

195 X. Sun, Y. Shi, W. Zhang, C. Li, Q. Zhao, J. Gao and X. Li, A new type Ni-MOF catalyst with high stability for selective catalytic reduction of NO_x with NH_3 , *Catal. Commun.*, 2018, **114**, 104–108.

196 Q. Wang, Q. Wang, B. Xu, F. Gao, F. Gao and C. Zhao, Flower-shaped multiwalled carbon nanotubes@nickel-trimesic acid MOF composite as a high-performance cathode material for energy storage, *Electrochim. Acta*, 2018, **281**, 69–77.

197 L. Zhang, Y. Zhang, S. Huang, Y. Yuan, H. Li, Z. Jin, W. Jiahao, Q. Liao, L. Hu, J. Lu, S. Ruan and Y. Zeng, $\text{Co}_3\text{O}_4/\text{Ni}$ -based MOFs on carbon cloth for flexible alkaline battery-supercapacitor hybrid devices and near-infrared photocatalytic hydrogen evolution, *Electrochim. Acta*, 2018, **281**, 189–197.



198 W. Zhu, C. Zhang, Q. Li, L. Xiong, R. Chen, X. Wan, Z. Wang, W. Chen, Z. Deng and Y. Peng, Selective reduction of CO_2 by conductive MOF nanosheets as an efficient co-catalyst under visible light illumination, *Appl. Catal., B*, 2018, **238**, 339–345.

199 H. T. T. Nguyen, D. N. A. Doan and T. Truong, Unprecedented salt-promoted direct arylation of acidic sp^2 C–H bonds under heterogeneous Ni-MOF-74 catalysis: synthesis of bioactive azole derivatives, *J. Mol. Catal. A: Chem.*, 2017, **426**, 141–149.

200 T. Q. N. Tran, G. Das and H. H. Yoon, Nickel–metal organic framework/MWCNT composite electrode for non-enzymatic urea detection, *Sens. Actuators, B*, 2017, **243**, 78–83.

201 C. Qu, Y. Jiao, B. Zhao, D. Chen, R. Zou, K. S. Walton and M. Liu, Nickel-based pillared MOFs for high-performance supercapacitors: design, synthesis and stability study, *Nano Energy*, 2016, **26**, 66–73.

202 T. Xu, X. Hou, S. Liu and B. Liu, One-step synthesis of magnetic and porous Ni@MOF-74(Ni) composite, *Microporous Mesoporous Mater.*, 2018, **259**, 178–183.

203 Y. Xu, A. J. Howarth, T. Islamoglu, C. T. D. Silva, J. T. Hupp and O. K. Farha, Combining solvent-assisted linker exchange and transmetallation strategies to obtain a new non-catenated nickel(II) pillared-paddlewheel MOF, *Inorg. Chem. Commun.*, 2016, **67**, 60–63.

204 L. Jiao, W. Yang, G. Wan, R. Zhang, X. Zheng, H. Zhou, S. H. Yu and H. L. Jiang, Single-Atom Electrocatalysts from Multivariate Metal–Organic, *Angew. Chem., Int. Ed.*, 2020, **59**, 20589–20595.

205 A. H. Wibowo, Y. I. F. Hasanah, M. Firdaus, D. M. Widjonarko and J. Cepeda, Efficient CO_2 adsorption by Cu(II) acetate and itaconate bioproduct based MOF, *J. Environ. Chem. Eng.*, 2018, **6**, 2910–2917.

206 Z. Wang, L. Ge, M. Li, R. Lin, H. Wang and Z. Zhu, Orientated growth of Copper-based MOF for acetylene storage, *Chem. Eng. J.*, 2019, **357**, 320–327.

207 J. Lincke, D. Lassig, J. Moellmer, C. Reichenbach, A. Puls, A. Moeller, R. Glaser, G. Kalies, R. Staudt and H. Krautscheid, A novel copper-based MOF material: Synthesis, characterization and adsorption studies, *Microporous Mesoporous Mater.*, 2011, **142**, 62–69.

208 G. Calleja, R. Sanz, G. Orcajo, D. Briones, P. Leo and F. Martinez, Copper-based MOF-74 material as effective acid catalyst in Friedel-Crafts acylation of anisole, *Catal. Today*, 2014, **227**, 130–137.

209 S. Bashkova and T. J. Bandosz, Effect of surface chemical and structural heterogeneity of copper-based MOF/graphite oxide composites on the adsorption of ammonia, *J. Colloid Interface Sci.*, 2014, **417**, 109–114.

210 F. Abbasloo, S. A. Khosravani, M. Ghaedi, K. Dashtian, E. Hosseini, L. Manzouri, S. S. Khorramrooz, A. Sharifi, R. Jannesar and F. Sadri, Sonochemical-solvothermal synthesis of guanine embedded copper based metal-organic framework (MOF) and its effect on *oprD* gene expression in clinical and standard strains of *pseudomonas aeruginosa*, *Ultrason. Sonochem.*, 2018, **42**, 237–243.

211 H. Mollabagher, S. Taheri, M. Mojtabaei and S. A. Seyedmousavi, Cu-metal organic frameworks (Cu-MOF) as an environment-friendly and economical catalyst for one pot synthesis of tacrine derivatives, *RSC Adv.*, 2020, **10**, 1995–2003.

212 J. Wang, A. S. Cherevan, C. Hannecart, S. Naghdi, S. P. Nandan, T. Gupta and D. Eder, Ti-based MOFs: new insights on the impact of ligand composition and hole scavengers on stability, charge separation and photocatalytic hydrogen evolution, *Appl. Catal., B*, 2021, **283**, 119626.

213 F. Cheng, Z. Li, L. Wang, B. Yang, J. Lu, L. Lei, T. Ma and Y. Hou, In situ Identification of Electrocatalytic Water Oxidation Behavior of Nickel-Based Metal–Organic Framework Nanoarray, *Mater. Horiz.*, 2021, **8**, 556–564.

214 X. Xuana, M. Qiana, L. Pan, T. Lu, L. Hanb, H. Yu, L. Wan, Y. Niua and S. Gong, Longitudinally Expanded Ni-Based Metal–Organic Framework with Enhanced Double Nickel Cation Catalysis Reaction Channels for Non-Enzymatic Sweat Glucose Biosensor, *J. Mater. Chem. B*, 2020, **8**, 9094–9109.

215 K. Wang, B. Lv, Z. Wang, H. Wu, J. Xua and Q. Zhang, Two-fold interpenetrated Mn-based metal–organic frameworks (MOFs) as battery-type electrode materials for charge storage, *Dalton Trans.*, 2020, **49**, 411–417.

216 M. Ganesh, P. Hemalatha, M. M. Peng, W. S. Cha and H. T. Jang, Zr-Fumarate MOF a Novel CO_2 -Adsorbing Material: Synthesis and Characterization, *Aerosol. Air Qual. Res.*, 2014, **14**, 1605–1612.

217 A. Kumar, M. Naushad, T. Ahamad and N. Viswanathan, Facile fabrication of tunable porous zirconium fumarate-based metal organic frameworks in the retention of nutrients from water, *Environ. Sci.: Water Res. Technol.*, 2020, **6**, 2856–2870.

218 A. Asghar, N. Iqbal, T. Noor, B. M. Kariuki, L. Kidwell and T. L. Easun, Efficient electrochemical synthesis of a manganese-based metal–organic framework for H_2 and CO_2 uptake, *Green Chem.*, 2021, **23**, 1220–1227.

219 H. Kaur, S. Sinha, V. Krishnan and R. R. Koner, Photocatalytic Reduction and Recognition of Cr(vi): New Zn(II)-Based Metal–Organic Framework as Catalytic Surface, *Ind. Eng. Chem. Res.*, 2020, **59**, 8538–8550.

220 G. Li, F. Li and J. Liu, Caimei Fan, Fe-based MOFs for photocatalytic N_2 reduction: key role of transition metal iron in nitrogen activation, *J. Solid State Chem.*, 2020, **285**, 121245.

221 F. Li, J. Li, L. Zhou and S. Dai, Enhanced OER performance of composite Co–Fe based MOF catalysts *via* a one-pot ultrasonic assisted synthetic approach, *Sustainable Energy Fuels*, 2021, **5**, 1095–1102.

222 N. Liu, Q. Q. Zhang and J. Guan, A binuclear Co-based metal–organic framework towards efficient oxygen evolution reaction, *Chem. Commun.*, 2021, **57**, 5016–5019.

223 Y. Li, X. Hu, X. Zhang, H. Cao and Y. Huang, Unconventional application of gold nanoclusters/Zn-MOF composite for fluorescence turn-on sensitive detection of zinc ion, *Anal. Chim. Acta*, 2018, **1024**, 145–152.

224 R. Pena-Rodriguez, J. A. Molina-gonzález, H. Desirena-Enriquez, J. M. Rivera-Villanueva and S. E. Castillo-Blum,



Tunable luminescence modulation and warm light emission of Zn-MOF (4,4'-bipyridyl and zinc acetate) doped with Eu³⁺ and Tb³⁺, *Mater. Chem. Phys.*, 2019, **223**, 494–502.

225 H. Duan, W. Dan and X. Fang, Zinc-coordinated MOFs complexes regulated by hydrogen bonds: synthesis, structure and luminescence study toward broadband white-light emission, *J. Solid State Chem.*, 2018, **260**, 159–164.

226 J. Zou, L. Li, S. You, H. Cui, Y. Liu, K. Chen, Y. Chen, J. Cui and S. Zhang, Sensitive luminescent probes of aniline, benzaldehyde and Cr(vi) based on a zinc(II) metal-organic framework and its lanthanide(III) post-functionalizations, *Dyes Pigm.*, 2018, **159**, 429–438.

227 K. Li, K. He, Q. Li, B. Xia, Q. Wang and Y. Zhang, A zinc(II) MOF based on secondary building units of infinite wavy-shaped chain exhibiting obvious luminescent sense effects, *Chin. Chem. Lett.*, 2019, **30**, 499–501.

228 I. T. Kim, S. Shin and M. W. Shin, Development of 3D interconnected carbon materials derived from Zn-MOF-74@carbon nanofiber web as an efficient metal-free electrocatalyst for oxygen reduction, *Carbon*, 2018, **135**, 35–43.

229 W. W. Lestari, M. Arvinawati, R. Martien and T. Kusumaningsih, Green and facile synthesis of MOF and nano MOF containing zinc(II) and benzene 1,3,5-tri carboxylate and its study in ibuprofen slow-release, *Mater. Chem. Phys.*, 2018, **204**, 141–146.

230 D. K. Yadav, V. Ganesan, F. Marken, R. Gupta and P. K. Sonkar, Metal@MOF Materials in Electroanalysis: Silver-Enhanced Oxidation Reactivity Towards Nitrophenols Adsorbed into a Zinc Metal organic Framework-Ag@MOF-5(Zn), *Electrochim. Acta*, 2016, **219**, 482–491.

231 S. Wang, Y. Lv, Y. Yao, H. Yu and G. Lu, Modulated synthesis of monodisperse MOF-5 crystals with tunable sizes and shapes, *Inorg. Chem. Commun.*, 2018, **93**, 56–60.

232 S. M. Mirsoleimani-azizi, P. Setoodeh, S. Zeinali and M. R. Rahimpour, Tetracycline antibiotic removal from aqueous solutions by MOF-5: adsorption isotherm, kinetic and thermodynamic studies, *J. Environ. Chem. Eng.*, 2018, **6**, 6118–6130.

233 H. A. Ozen and B. Ozturk, Gas separation characteristic of mixed matrix membrane prepared by MOF-5 including different metals, *Sep. Purif. Technol.*, 2019, **211**, 514–521.

234 K. G. Liu, Z. Sharifzadeh, F. Rouhani, M. Ghorbalnoo and A. Morsali, Metal-organic framework composites as green/sustainable catalysts, *Coord. Chem. Rev.*, 2021, **436**, 213827.

235 Y. Y. Kannangara, U. A. Rathnayake and J. Song, Redox active multi-layered Zn-pPDA MOFs as high-performance supercapacitor electrode material, *Electrochim. Acta*, 2019, **297**, 145–154.

236 Y. Wu, H. Pang, W. Yao, X. Wang, S. Yu, Z. Yu and X. Wang, Synthesis of rod-like metal-organic framework (MOF-5) nanomaterial for efficient removal of U(vi): batch experiments and spectroscopy study, *Sci. Bull.*, 2018, **63**, 831–839.

237 Y. Z. Chen, Z. U. Wang, H. Wang, J. Lu, S. H. Yu and H. L. Jiang, Singlet Oxygen-Engaged Selective Photo-oxidation over Pt Nanocrystals/Porphyrinic MOF: The Roles of Photo-thermal Effect and Pt Electronic State, *J. Am. Chem. Soc.*, 2017, **139**, 2035–2044.

